SEMMELWEIS EGYETEM

DOKTORI ISKOLA

Ph.D. értekezések

2726.

BERECZ TÜNDE

Szív- és érrendszeri betegségek élettana és klinikuma
című program

Programvezető: Dr. Merkely Béla, egyetemi tanár

Témavezetők: Dr. Apáti Ágota, tudományos főmunkatárs

Dr. Földes Gábor, egyetemi docens

DISEASE MODELING USING INDUCED PLURIPOTENT STEM CELL DERIVATIVES

PhD thesis

Tünde Berecz

Basic and Translational Medicine Doctoral School

Semmelweis University

Supervisors: Ágota Apáti, PhD

Gábor Földes, MD, DSc

Official reviewers: Nándor Nagy, PhD

Tamás Bálint Csont, MD, PhD

Head of the Complex Examination Committee: Tivadar Tulassay, MD, Member of the Hungarian Academy of Sciences

Members of the Complex Examination Committee: Attila Patócs, MD, DSc

Péter Andréka, MD, PhD

Budapest

2022

Table of contents

List of abbreviations

22q11.2DS – 22q11.2 deletion syndrome

AMPA – α-amino-3-hydroxy-5-methyl-4-isoxazolepropionic acid

AP2α/TFAP2A – transcription factor AP-2 alpha

ATP – adenosine triphosphate

BMP – bone morphogenetic protein

BMP4 – bone morphogenetic protein 4

CGH – comparative genomic hybridization

CHARGE – coloboma, heart defects, atresia choanae, growth retardation, genital abnormalities, and ear abnormalities

CHD – congenital heart disease

CMs – cardiomyocytes

c-MYC – MYC proto-oncogene, BHLH transcription factor

cNNCs – cardiac neural crest cells

CNS – central nervous system

DG – dentate gyrus

ECM – extracellular matrix

eGFP – enhanced green fluorescent protein

EGTA – ethylene glycol-bis(β-aminoethyl ether)-N,N,N′,N′-tetraacetic acid

EMT – epithelial to mesenchymal transition

ER – endoplasmic reticulum

FACS – fluorescence-activated cell sorting

FGF – fibroblast growth factor

FISH – fluorescent in situ hybridization

GJA1/Cx43 – gap junction protein alpha 1

GJA5/Cx40 – gap junction protein alpha 5

HCN4 – hyperpolarization activated cyclic nucleotide gated potassium channel 4

hESCs – human embryonic stem cells

hiPSC-CMs – human induced pluripotent stem cell-derived cardiomyocytes

hiPSC-NCCs – human induced pluripotent stem cell-derived neural crest cells

hiPSC-NPCs – human induced pluripotent stem cell-derived neural progenitor cells

hiPSCs – human induced pluripotent stem cells

hPSCs – human pluripotent stem cells

IP_3 – inositol 1,4,5-trisphosphate

IP_3R – inositol 1,4,5-trisphosphate receptor

iPSCs – induced pluripotent stem cells

KCl – potassium chloride

KLF4 – Kruppel-like factor 4

LATS1/2 – large tumor suppressor kinase 1/2

LCRs – low copy repeats

LIN-28 – Lin-28 homolog A

LPA – lysophosphatidic acid

$LPAR_{1-4}$ – lysophosphatidic acid receptor 1-4

MCU – mitochondrial calcium uniporter

MEF - mouse embryonic fibroblast

MEF2C – myocyte enhancer factor 2C

MLPA – multiplex ligation-dependent probe amplification

MNCX – mitochondrial Na^+/Ca^{2+} exchange

MOB1A/1B – MOB kinase activator 1A/1B

MTS1/2 – STE20-like protein kinase 1/2

MYL2 – myosin light chain 2

MYL7 – myosin light chain 7

NANOG – homeobox transcription factor Nanog

NC – neural crest

NCCs – neural crest cells

NCX – Na^+/Ca^{2+} exchange

NGFR/P75 – nerve growth factor receptor

NMDA – N-methyl-D-aspartate

NPC – neural progenitor cell

NSCC – non-selective cation-current

OCT3/4 – POU class 5 homeobox 1

OFT – outflow tract

PAR2 – protease activated receptor 2

PBMC – peripheral blood mononuclear cells

PIP_2 – phosphatidylinositol 4,5-bisphosphate

PMCA – plasma membrane Ca^{2+} ATPase

PROX1 – Prospero Homeobox 1

RA – retinoic acid

RyR – ryanodine receptor

SAV1 – Salvador family WW domain containing protein 1

SERCA – sarco/endoplasmic reticulum Ca^{2+} ATPase

SOCE –store operated calcium entry

SOX10 – SRY-box transcription factor 10

SOX2 – SRY-box transcription factor 2

SOX9 – SRY-box transcription factor 9

SSEA-4 – stage-specific embryonic antigen 4

TAZ – transcriptional co-activator with PDZ-binding motif

TBX1 – T-box transcription factor 1

TEAD – transcriptional enhancer associate domain

TMRM – tetramethylrhodamine, methyl ester

TNNI3 – troponin I3, cardiac type

TOF – tetralogy of Fallot

VGCC – voltage-gated calcium channel

VSD – ventricular septal defect

VSMCs – vascular smooth muscle cells

WES – whole exome sequencing

Wnt – wingless-type MMTV integration site family

YAP – Yes-associated protein

1. Introduction

Cardiovascular and neurological diseases are the most common causes of death worldwide [1, 2], strongly motivating the study of the cause and mechanisms leading to the development of these diseases. This thesis focuses on how to use human induced pluripotent stem cell-derivatives for disease modeling, especially when the disease affected cell types are hardly accessible such as cardiomyocytes or neural cell types.

1.1. Classification of stem cells

Meanwhile the main purpose of symmetric cell division (when the two daughter cells are identical) is proliferation, a key characteristic of stem cells is asymmetric cell division, when one of the daughter cells is identical to the origin (thus maintaining the stem cell pool), and the other becomes committed to a more specified cell fate [3, 4].

Four types of stem cells are classified based on their differentiation potential: totipotent, pluripotent, multipotent and unipotent [5] (Fig.1). Totipotent stem cells are formed after fertilization, when the zygote divides into cells in the morula stage of development. Totipotent stem cells can give rise to all cell types of the human body. These cells develop further into the blastula stage, where the inner cell mass part of the blastocyst contains pluripotent stem cells. Pluripotent stem cells can give rise to all cell types of the human body, excluding the extraembryonic tissues [6]. Multipotent stem cells are generated from these cells committed to lineage-specific differentiation, having the potential to differentiate into a limited number of cell types. With further specification, unipotent stem cells are formed with the ability to differentiate into one specific cell type exclusively. Even though they start to form during prenatal development, multipotent and unipotent stem cells are called adult stem cells (also called tissue-specific stem cells or somatic stem cells) and are found in the body throughout the majority of postnatal life as well [7].
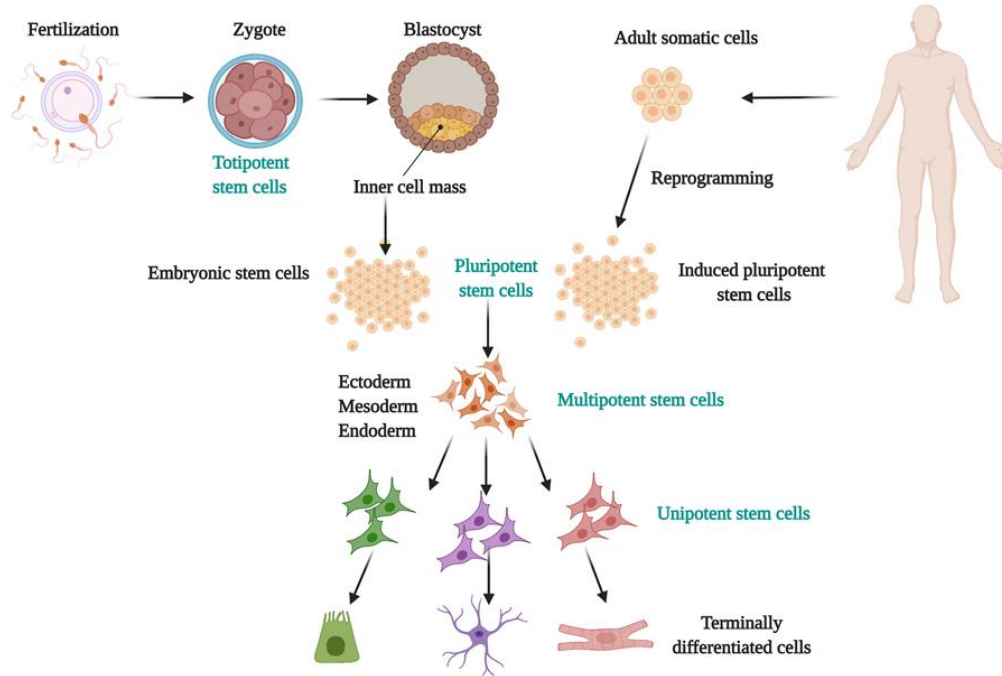
Figure 1. **Classification of stem cells** (See description in the text)

(Figure generated using BioRender)

1.2. Human pluripotent stem cells

The source of human pluripotent stem cells (hPSCs) can be i) human embryonic stem cells (hESCs) originating from the inner cell mass of the blastocyst stage of the embryo, and ii) human induced pluripotent stem cells (hiPSCs) obtained from adult somatic cells via genetic reprogramming (Fig.1.). hESCs and hiPSCs are considered equivalents in terms of pluripotency. hPSCs have the ability of unlimited cell division while maintaining their pluripotency and self-renewal. Under well-defined *in vitro* conditions, hPSCs thus offer unlimited cell sources for numerous applications. hPSCs and their differentiated derivatives are widely used for disease modeling, toxicology testing and drug development, and provide promising regenerative medicine opportunities [8, 9].

1.2.1. Generation of human induced pluripotent stem cells

The first induced pluripotent stem cells (iPSCs) were generated from mouse fibroblasts by the research group of Shinya Yamanaka in 2006 [10], and subsequently, the first hiPSCs were derived from human fibroblasts in 2007 [11]. The "classical" genetic reprogramming occurs through the forced expression of four genes, also called the Yamanaka factors: POU

class 5 homeobox 1 (OCT3/4, also known as POU5F1), SRY-box transcription factor 2 (SOX2), Kruppel-like factor 4 (KLF4) and MYC proto-oncogene, BHLH transcription factor (c-MYC). During the same time, the Thomson group independently generated hiPSCs from human fibroblasts using OCT3/4, SOX2, homeobox transcription factor Nanog (NANOG) and Lin-28 homolog A (LIN-28) [12]. In the process of reprogramming, these factors reactivate endogenous transcription factors responsible for the initiation and maintenance of pluripotency. Further maintenance of pluripotency does not require the presence of reprogramming transgenes [13].

Initially, fibroblasts isolated from skin biopsies were the most commonly used cell source for hiPSC generation. However, this has been replaced with less invasive approaches, such as cells isolated from peripheral blood or urine [14].

The reprogramming genes can be introduced into the cells by various methods [15, 16]. Retroviral and lentiviral vectors were used to establish the first hiPSCs [11, 12], which are still among the most efficient and reproducible gene delivery methods. However, these approaches require the integration of transgenes into the host genome, possibly leading to the disruption of genome integrity. Removal of the transgenes from the host genome after the reprogramming process (e.g. using Cre/lox [17] or piggyBac transposon system [18]) is a possible solution, still it makes the reprogramming system more complicated. Adenoviral vectors do not integrate into the genome, but the obtained efficiency of reprogramming is lower compared to integrating viral vectors [19]. On the other hand, Sendai virus is a non-integrating RNA virus vector providing transient expression of the reprogramming factors combined with high reprogramming efficiency [20]. Nucleofection of plasmid vectors or episomal vectors carrying the reprogramming genes is another non-integrating approach for transient expression, but shows low reprogramming efficiency [21]. Furthermore, there are non-genetic reprogramming approaches, e.g. instead of genes, delivering the mRNA [22] or recombinant protein of the corresponding transcriptions factors [23] into the cells. While the mRNA method can be a promising tool, delivery of transcription factor proteins through the plasma membrane is cumbersome due to the size of these proteins.

Overall, the reprogramming techniques have become available for research purposes, and the usage has been increasing greatly, with Sendai virus-based delivery system being the most popular reprogramming method [24].

1.2.2. Disease modeling with human pluripotent stem cells

hPSCs and their differentiated derivatives provide promising opportunities for studying disease-related phenotypes *in vitro*. These approaches are particularly important when human cell types cannot be investigated directly or in the long-term, or no appropriate animal models are available [25, 26]. Studying differentiation and cell maturation processes can provide insights into disease development and lead us to identify possible targets for treatment.

In vitro modeling systems for environmental factor induced diseases, pharmacological factor-induced or stress-induced diseases use healthy cell lines to recapitulate the harmful effects of a certain agent or stress factors. These systems are used to discover cellular and molecular level mechanisms aiming to help the development of preventive strategies and treatment.

Finally, modeling genetic diseases requires cells with pathogenic genetic alterations. These cells are obtained either by genetic manipulation of wild-type cell lines (e.g. generating a mutation of interest) or by establishing cell lines originating from patients carrying genetic alterations. In certain cases, the disease-associated genetic background can be corrected by gene-editing tools to generate isogenic control cells, or to test if correction of the given gene rescues the phenotype [27, 28].

1.3. Differentiation methods for generating relevant cell types for disease modeling

1.3.1. Cardiomyocyte differentiation from hiPSCs

Cardiomyocytes are the main cell type building up the myocardium of the heart located in the walls of the four chambers, in the septa, and the papillary muscle connecting to the mitral valves [29] (Fig. 2. C). Since the heart is the first functioning organ to develop in the embryo [30], it is not surprising that the mesoderm-derived beating cardiac cells are among the first emerging cell types in spontaneous differentiation of hPSCs *in vitro*. These cardiac cells are surrounded by many other cell types in a spontaneously differentiating cell culture, representing derivatives of all three germ layers. To increase the ratio of cardiomyocytes in the cell culture or generate pure cardiac cell cultures, directed differentiation methods had to be developed. The first protocol for generating cardiomyocytes from hPSCs was reported in 2001, starting differentiation from embryoid bodies using serum but achieving low

differentiation efficiency (5-10%) [31]. To increase efficiency, several other methods have been reported. Co-culture with mouse endoderm-like cells increased cardiac differentiation efficiency [31], with the compromise of having multiple cell types from different species in the studied cell culture. The major signaling pathways determining cardiomyogenesis include bone morphogenetic protein (BMP), Nodal/Activin, wingless-type MMTV integration site family (Wnt), fibroblast growth factor (FGF) and Notch [32, 33]. Using cytokines, such as Activin A and bone morphogenetic protein 4 (BMP4), and hormones, such as insulin for the induction of cardiac differentiation brought significant improvements in differentiation efficiency [34]. To note, insulin inhibits cardiac mesoderm formation [35], but improves the subsequent yield of differentiated cardiomyocytes by increasing cell survival and proliferation [36]. These factors were successfully applied for cardiac myocyte induction both in 3D embryoid body-based systems and in 2D monolayer cell cultures. As a next step, applying small molecules modulating signaling pathways made it possible to establish serum-free, xeno-free, cytokine- and hormone-free differentiation protocols [37]. To improve cardiomyocyte purity, several purification methods have been developed, such as i) metabolic selection based on glucose retrieval from the culturing media and supplementation with lactate, ii) fluorescence activated cell sorting (FACS) based on high mitochondrial activity or using molecular beacons (nano-sized probes for specific mRNAs), or iii) separation of labeled un-differentiated cells in microfluidic system [38]. Generally, hPSC-derived cardiomyocyte differentiation protocols yield in a mixed population of atrial, ventricular and pacemaker-like cells. However, the recent emergence of subtype-specific differentiation protocols makes it possible to generate homogenous populations [39]. hPSC-derived cardiomyocytes (hPSC-CMs) resemble fetal cardiac cells, regarding gene expression, sarcomere structure, metabolism and electrophysiological characteristics. Indeed, even in mixed populations, hPSC-CMs show spontaneous contractile activity (not restricted to nodal-like cells only), which is a characteristic of fetal-like cardiac cells. Maturation techniques for the generation of more adult-like cardiomyocytes have been published, and are shown to be more suitable for certain disease modeling approaches and toxicology testing platforms [39, 40]. Prolonged culturing time is an obvious option, but other approaches have also been developed because it is time-consuming and longer maintenance is more expensive. Cardiomyocytes switch metabolic state prenatally and during *in vitro*

maturation from glycolysis to oxidative phosphorylation [41, 42], indicating that glucose retrieval, along with its beneficial effect on purity, can help the metabolic maturation of cardiac cells [41]. Mechanical [43] and/or electrical stimuli [44] improve sarcomere structure maturation and electrophysiological properties. Applying fluid flow inducing shear stress also has a beneficial effect on cardiac maturation [45]. On the other hand, while cardiomyocyte maturity is important for modeling adult-onset cardiac diseases [46], investigating the early steps of cardiomyogenesis can be very informative in developmental disease modeling. Studying differentiation in immature, fetal-like cardiac cell types is crucial for understanding the underlying mechanisms of congenital cardiac diseases. Additionally, considering that the regenerative capacity of the adult human heart is known to be limited, application of more immature cells with higher proliferative capacity could be beneficial for regenerative treatment as well, however, spontaneous contractility raises concerns about the risk of arrhythmia [47].

1.3.2. Cardiac neural crest cells

Neural crest cells (NCCs) are ectodermal in origin and arise from the dorsal neural tube (Fig. 2. A). Depending on the segment of the anterior-posterior axis, they are classified as cranial, cardiac, vagal, and trunk NCCs [48]. Premigratory neural crest cells undergo epithelial to mesenchymal transition (EMT) and migrate to different embryonic tissues following specific cues. When NCCs reach their destination, they give rise to a variety of cell types, such as osteoblasts and chondrocytes in the head, smooth muscle cells in the great vessels and cardiac septa, sympathetic and parasympathetic neurons of the peripheral nervous system, chromaffin cells of the adrenal gland, and melanocytes in the skin [49].

Cardiac neural crest cells (cNCCs) originate from between the mid-otic placode and the third somite [50], and migrate through the 3rd, 4th and 6th pharyngeal arches to the developing heart (Fig. 2. B), where they become part of the cardiac mesenchyme and differentiate into smooth muscle cells [51-53]. A portion of cNCCs remains in the arch arteries playing a role in forming the great arteries, specifically having a role in aorticopulmonary septation and aortic arch remodeling. Another part of cNCCs migrate to the developing cardiac outflow tract (OFT), assisting in its formation and playing a role in OFT cushion remodeling forming the semilunar valves [51, 54]. Additionally, cNCCs migrate to the endocardial cushions, where

they are required to form the membranous intraventricular septum. They contribute to the smooth muscle of the coronary arteries as well [55] (Fig. 2. C).

Defects in the differentiation of cNCCs into VSMCs have been indicated to cause various cardiovascular disorders, including OFT anomalies, and ventricular septal defect (VSD) or tetralogy of Fallot (TOF) supposedly caused by malalignment between the OFT and the ventricles during cardiac looping [56].

In general, defects in neural crest differentiation and specification, disrupted migration, impaired viability or self-renewal capacity or improper differentiation capacity cause neurocristopathies [57], and those affecting cNCCs can lead to abnormal cardiovascular development, e.g. seen in coloboma, heart defects, atresia choanae, growth retardation, genital abnormalities, and ear abnormalities (CHARGE) syndrome, DiGeorge syndrome or Treacher Collins syndrome [50, 58, 59]. Cardiac neural crest ablation studies showed abnormal looping and induced cardiovascular abnormalities in animal models [50, 60-62]. However, the exact mechanisms of how improper NC development causes congenital heart defects are still not clearly understood.

1.3.3. Neural crest cell differentiation from hiPSCs

NCC induction is regulated by BMP, Wnt, Notch, and FGF signaling. Addressing these molecular pathways, protocols for the generation of human NCCs started to emerge in 2005 [49, 63, 64]. NCC induction approaches involved stromal cell co-culture, and later 3D neurosphere or monolayer induction of neural rosettes. These protocols result in a mixed population of neural precursors and neural crest cells followed by a subsequent enrichment of migratory NCCs [49]. Another interesting approach is transcription factor-based reprogramming of fibroblasts with a single transcription factor SRY-box transcription factor 10 (SOX10) [65]. The most recent protocols aim to achieve directed and specific NCC induction from hPSCs in defined adherent culture using small molecules [66, 67]. Although, 3D spheroid-based protocols using differentiation factors, such as FGF and Activin A, are still used [68, 69]. Protocols aiming to define certain regional NCC identity have also emerged using BMP4 or retinoic acid (RA) to direct anterior or posterior NCC specification [70, 71] however, specific cNCC producing protocols are yet to be developed.
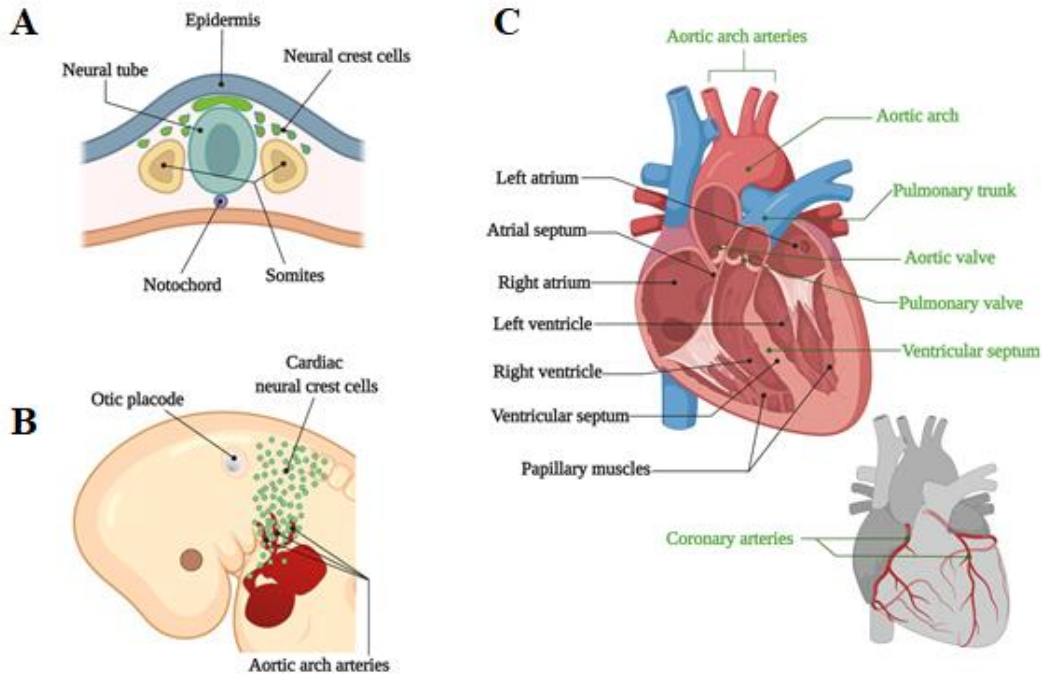
Figure 2. **Cardiac neural crest cells contribute to cardiovascular development**

(A) Neural crest cells originate from the dorsal neural tube. (B) Cardiac neural crest cells migrate to the developing heart. (C) Human adult myocardium (black labels) and parts of the cardiovascular system with neural crest contribution (green labels).

(Figure generated using BioRender)

1.4. Background for hiPSC-derived disease models

In this thesis, I demonstrate two examples of how to use hiPSC-derivatives for disease modeling. The first model aims to investigate Hippo pathway-YAP/TAZ signaling in doxorubicin-induced cardiotoxicity, as an example for modeling drug-induced disease. The second model aims to study DiGeorge syndrome, a complex genetic disease, focusing on the cardiovascular aspects of DiGeorge syndrome, and providing the basis for further study of the neural crest and neural aspects of the disease.

1.4.1. Hippo pathway-YAP/TAZ signaling in doxorubicin induced cardiotoxicity

Anthracyclines are highly effective drugs particularly used against breast cancer and hematological malignancies [72, 73]. On the other hand, these drugs are the leading cause of cardiac dysfunction in cancer survivors [74]. Doxorubicin has a multimodal mechanism of

inducing cardiotoxicity, including impairment of mitochondrial metabolism, production of reactive oxygen species, disruption of Ca^{2+} modulation and direct DNA damage [75]. Since the regenerative potential of cardiac cells is known to be low [76], controlling cell survival in cardiomyocytes is more important than in cell types with greater regenerative capacity. Hippo signaling is an evolutionarily conserved pathway controlling organ size by regulating cell proliferation, apoptosis, and stem cell self-renewal [77, 78]. In humans, STE20-like protein kinase 1/2 (MTS1/2, ortholog of Drosophila Hippo), large tumor suppressor kinase 1/2 (LATS1/2), and their respective adaptor proteins MOB kinase activator 1A/1B (MOB1A/1B) and Salvador family WW domain containing protein 1 (SAV1) form a core kinase cascade (Fig. 3.). The physiological output of this kinase cascade is the regulation of the key effectors of the Hippo pathway, Yes-associated protein (YAP) and transcriptional co-activator with PDZ-binding motif (TAZ). When the canonical Hippo pathway is active, the core kinase cascade phosphorylates YAP/TAZ, leading to cytoplasmic retention. Phosphorylated YAP/TAZ is either bound to 14-3-3 protein and sequestrated in the cytoplasm, or ubiquitinated leading to proteasomal degradation. YAP/TAZ is dephosphorylated and translocated into the nucleus when the Hippo pathway is inactive. It interacts with transcriptional enhancer associate domain 1-4 (TEAD1-4) and other transcription factors as transcriptional co-activators promoting proliferation and inhibition of cell death.
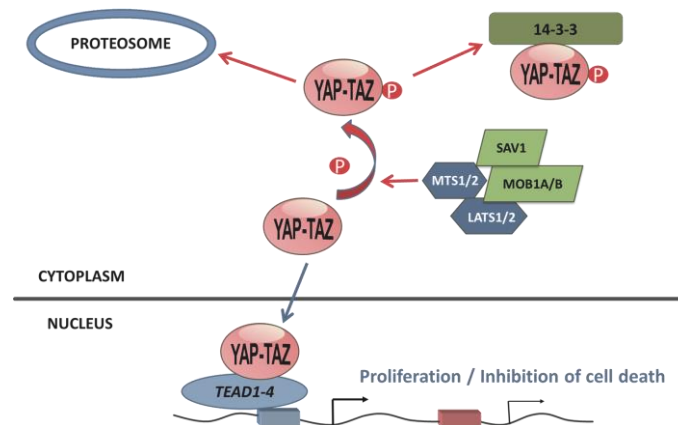

Figure 3. **YAP/TAZ core module** (See description in the text)

Dysregulation of the Hippo pathway, via activation of YAP and TAZ, results in uncontrolled proliferation and suppression of apoptosis in adult organs, and it has been implicated in

tumorigenesis of breast, colon, lung, and liver cancers [79-81]. Small molecule YAP inhibitors are a potential new therapeutic strategy for various cancers [79, 80]. Hippo pathway has also been shown to play a crucial role in regulating cardiomyocytes [82]. In adult hearts, YAP silencing led to dilated cardiomyopathy and overexpression of YAP increased cardiomyocyte number and thus heart size in mouse models [83]. Moreover, when YAP is overexpressed in the adult mouse heart, enhanced preservation of heart function and reduced scar size was observed after myocardial infarction [84]. Consistent with the *in vivo* observation of doxorubicin-induced reduction of heart size in mice [85], doxorubicin treatment decreased the expression of YAP and caused cell death of neonatal and H9c2 rat cardiomyocytes *in vitro* [86, 87]. In contrast, overexpression of YAP inhibited doxorubicin-induced cardiac cell loss *in vitro* [87]. These findings suggest that YAP/TAZ activation is modified in response to doxorubicin treatment and is a promising potential target for regenerative or protective therapy of the heart [88].

Hippo pathway and YAP/TAZ transcriptional co-activators in doxorubicin-induced cardiotoxicity have previously been characterized in H9c2 rat cardiac cells and animal models [85, 88, 89]. In this thesis, I present the first human-based study addressing Hippo pathway and YAP/TAZ transcriptional co-activators in doxorubicin-induced cardiotoxicity. Our previous results showed that based on RNA sequencing data of *ex-vivo* human heart samples evaluating key signaling pathways in doxorubicin-induced cardiotoxicity, YAP is an upstream regulator of genes found to be differentially expressed in samples from patients with doxorubicin-induced heart failure as compared to healthy controls [90]. Since hPSC-CMs are suitable for characterization of molecular mechanisms of cardiotoxicity [75, 91], we generated a human *in vitro* model for doxorubicin-induced cardiotoxicity for the investigation of the role of YAP/TAZ.

1.4.2. DiGeorge syndrome

DiGeorge syndrome, also called 22q11.2 deletion syndrome (22q11.2DS) or velocardiofacial syndrome, is the most common microdeletion syndrome with a prevalence of 1:3000 – 1:6000 in live births, and based on invasive prenatal testing, the occurrence is 1:1000 in fetuses. The genetic background of the disease is a monoallelic microdeletion on chromosome 22 caused by meiotic chromosomal rearrangements due to non-allelic

homologous recombination. Approximately 95 % of the cases are *de novo* deletions, and in 5 % of the cases is the disease inherited in an autosomal dominant manner [92]. The specific vulnerability of the 22q11.2 region to meiotic errors is due to four low copy repeats (LCRs), namely LCR22A, LCR22B, LCR22C and LCR22D. LCRs are highly similar, large blocks of segmental duplications. Deletions of different sizes can occur between LCRs. In over 90 % of the patients the typical 3 Mb long deletion affecting more than a hundred genes is found, while atypical deletions are smaller.

Hemizygosity of the affected genes leads to haploinsufficiency, meaning that one copy of the genes is insufficient for the healthy phenotype. 22q11.2 deletion causes a heterogeneous presentation of clinical symptoms, affecting several organ systems. Congenital defects in DiGeorge syndrome are considered to emerge due to perturbation of the pharyngeal region during embryogenesis.

22q11.2 deletion is one of the most common causes of congenital heart disease (CHD) and developmental delays [92]. 64 % of patients develop CHD. The most frequent cardiac defects are interrupted aortic arch, truncus arteriosus, tetralogy of Fallot (TOF), ventricular septal defects and vascular rings [92, 93]. TOF consists of overriding or misplaced aorta, ventricular septal defect, pulmonary valve stenosis or pulmonary atresia, and right ventricular hypertrophy. Pentalogy of Fallot occurs when TOF is combined with atrial septal defect [94]. Low blood oxygen level (due to TOF or ventricular and/or atrial septal defect) leads to cyanosis. Cognitive deficit, learning disability, behavioral difficulty and mental illness are very common in DiGeorge syndrome. Approximately 30 % of the patients develop schizophrenia [95] and 30-40 % suffer from autism spectrum disorder [96]. Immunodeficiency also affects up to 75 % of the patients due to the absence of thymus or thymic aplasia and autoimmune diseases are also common. Hypoparathyroidism or absence of parathyroid glands are frequent, leading to hypocalcemia. Other typical congenital features are craniofacial malformations, palatal abnormalities (e.g. cleft palate), breathing problems due to airway malformation, swallowing difficulties and gastrointestinal problems, and renal and skeletal anomalies. Premature mortality is frequent [92].

The affected organ systems vary among patients, and the range of symptoms is broad, from mild to severe clinical manifestations. Interestingly, the highly variable phenotypic expression and severity of symptoms are not correlated with the size of the deletion, but

severity usually increases when inherited [97]. Proposed mechanisms underlying the heterogeneous clinical manifestations with same size 22q11.2 deletion are: i) gene dosage effect (changes in the copy number of the gene affects the amount of gene product), ii) gene variants on the intact allele within the 22q11.2 region, iii) other gene variants outside the 22q11.2 region and iv) epigenetic and environmental factors.

On the typical 3 Mb long 22q11.2 region approximately 106 genes are found, including 46 protein-coding genes, 7 microRNA and 12 long non-coding RNA genes, 2 small nucleolar RNA genes, 27 pseudogenes, and additional predicted coding and non-coding genes [93, 98]. In spite of that there are mouse models [99-102], generating the appropriate animal model recapitulating all the specific human features of the disease is difficult due to the different genetic organization of the locus and missing orthologue genes in mice [93]. hiPSC-based models have the key advantage of providing the complicated genetic background of the disease. There has been only one study focusing on the cardiovascular aspects, reporting that T-box transcription factor 1 (TBX1) regulates myocyte enhancer factor 2C (MEF2C) expression levels (an important cardiac differentiation transcription factor) in a dosage-dependent manner [103].

Most of the currently published hiPSC-based models for DiGeorge syndrome focus on the neural aspects of the disease [96, 104-109]. Calcium deficit has been shown in 3 dimensional cortical organoids and 2 dimensional cortical neurons differentiated from hiPSCs of 22q11.2DS patients [96]. Altered gene expression and function of hippocampal dentate granule neurons in 22q11.2DS has been shown in mouse models [110, 111]. However, there has been no human-based model studying the involvement of these cells in DiGeorge syndrome.

1.4.3. Calcium signaling in hippocampal dentate gyrus granule cells

The dentate gyrus (DG) is the only known region of the human brain where neurogenesis persists into adulthood [112, 113]. New neurons generated in the DG are essential for learning, pattern separation, and spatial memory formation [114], and alterations of hippocampal neurogenesis have been implicated in several disease conditions, including schizophrenia [115-119], epileptic seizures [120], Alzheimer's disease [121] and cognitive defects characteristic of depression [122, 123]. Since animal models are often inefficient in

recapitulating human central nervous system (CNS) disorders, the generation of proper human cell-based systems has been proposed for both disease-modeling and drug screening purposes. Neurons differentiated from hPSCs using various protocols, e.g. specific morphogenic patterning cues, show characteristics of multiple neuronal subtypes [124-126]. This heterogeneity can already be monitored at the progenitor state [127, 128]. A protocol has been developed to generate hPSC-derived neural progenitor cells (NPCs) that preferentially differentiate into a cell population enriched in hippocampal DG granule cells expressing Prospero Homeobox 1 (PROX1) [129], a specific marker of this cell type [130, 131]. It was shown that directed differentiation to hippocampal granule neurons could reveal disease-related phenotypes in hiPSC models of schizophrenia [129] and bipolar disorder [132].

Calcium ions, as ubiquitous intracellular messengers, play a fundamental role in numerous cellular processes, including proliferation, differentiation, and excitability. The measurement of neuronal calcium signaling has recently become an important tool to study calcium channel activity, intracellular calcium release, as well as calcium-dependent neurotransmitter release in *in vitro* cultured NPCs and neurons [127, 133-136]. Calcium signals are highly variable during long-term culturing of NPCs [127], therefore, ligand-induced calcium transients may be predictive of their ability to generate mature neurons. We applied adenosine triphosphate (ATP), lysophosphatidic acid (LPA), and trypsin as ligands to evoke calcium signals. ATP binds to purinergic receptors P_2X plasma membrane ion channel receptor leading to calcium influx from the extracellular space [137], and P_2Y 7-transmembrane G protein-coupled receptor leading to intracellular Ca^{2+} release through inositol 1,4,5-trisphosphate (IP_3) signaling [138]. LPA and trypsin bind to 7-transmembrane G protein-coupled receptors lysophosphatidic acid receptor 1-4 ($LPAR_{1-4}$) and protease activated receptor 2 (PAR2) respectively [139, 140]. The activated Gαq subunit activates phospholipase C-β; an enzyme in the plasma membrane catalyzing the conversion of phosphatidylinositol 4,5-bisphosphate (PIP_2) to diacylglycerol and IP_3. IP_3 binding to inositol 1,4,5-trisphosphate receptor (IP_3R) ion channel receptor in the endoplasmic reticulum (ER) causes calcium release from the ER (Fig. 4.) [141, 142]. The increased Ca^{2+} level is subsequently restored by several mechanisms. Sarco/endoplasmic reticulum Ca^{2+} ATPase (SERCA) and plasma membrane Ca^{2+} ATPase (PMCA) are responsible for pumping Ca^{2+}

from the cytoplasm to the ER or to the extracellular space respectively [143]. Other mechanisms through the plasma membrane are store operated calcium entry (SOCE) [144], Na^+/Ca^{2+} exchange (NCX) [145], non-selective cation-current (NSCC) [146] and in excitatory cells voltage-gated Ca^{2+} channels (VGCC) [147]. Cytoplasmic Ca^{2+} level is also regulated by the mitochondria through mitochondrial calcium uniporter (MCU) [148] and mitochondrial Na^+/Ca^{2+} exchange (MNCX) [149]. Additionally, Ca^{2+} diffuses freely between the cytoplasm and nucleus through the nuclear pore complexes [150].
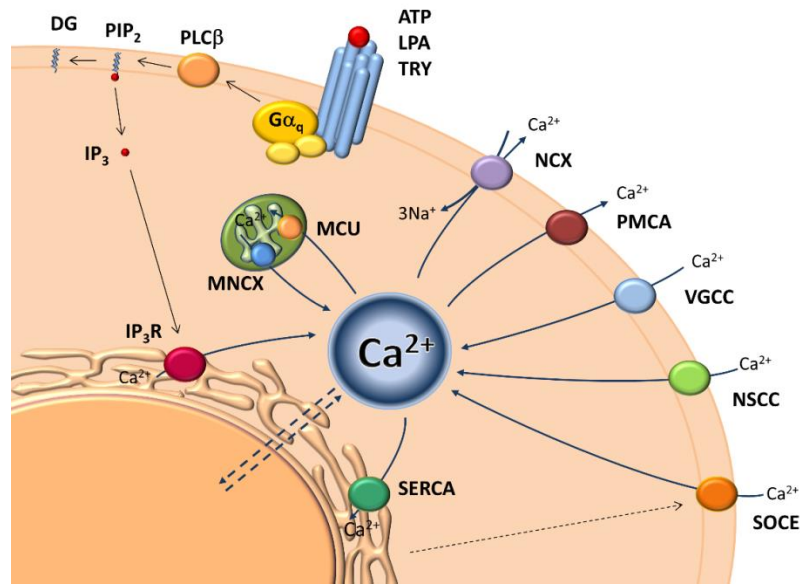

Figure 4. **Regulation of cytoplasmic calcium level** (See description in the text)

In neurons, cytoplasmic Ca^{2+} originates both from internal Ca^{2+} stores regulated by IP_3R and ryanodine receptor (RyR) [151-154], and from the extracellular space primarily regulated by ligand-specific channels; such as glutamate receptors, or by voltage-gated Ca^{2+} channels (VGCC) [147]. Granule neurons are excitatory glutamatergic neurons in the DG [155, 156]. Among the receptors of glutamate excitatory neurotransmitter, α-amino-3-hydroxy-5-methyl-4-isoxazolepropionic acid (AMPA) and N-methyl-D-aspartate (NMDA) receptors take part in the increase of cytoplasmic Ca^{2+} levels [157, 158] (Fig. 5). AMPA and NMDA receptors are localized in the same synapse in a close vicinity to each other [159]. Na^+ influx evoked by the activation of AMPA receptor causes depolarization. Membrane depolarization

leads to the release of Mg^{2+} from NMDA receptors, giving way to Ca^{2+} through glutamate-bound NMDA receptors.
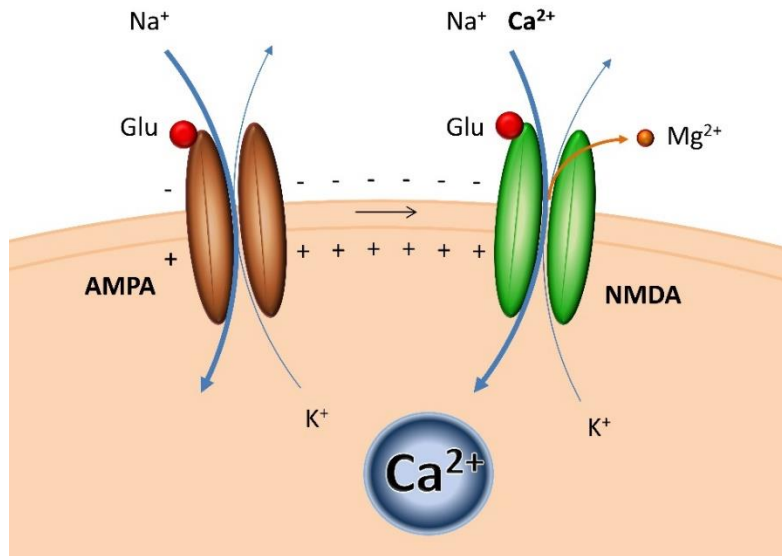

Figure 5. **Glutamate receptors in neurons** (See description in the text)

2. Objectives

This thesis work aims to generate hiPSC-based *in vitro* models for better understanding cellular and molecular level disease mechanisms aiming to help the development of preventive strategies and treatment. Specifically, in this thesis, I present two disease models; i) a drug-induced disease and ii) a genetic disease.

Our previous RNA sequencing analysis of human myocardial samples of patients with doxorubicin-induced heart failure showed that YAP is an upstream regulator of differentially expressed genes [90]. Several mechanisms in doxorubicin-induced cardiotoxicity have been reported in human cells [160], but there has been no human-based model studying the role of YAP/TAZ. In this study, by using hiPSC-derived cardiomyocytes (hiPSC-CMs), I aim to answer the following questions:

1. What is the mechanism for doxorubicin-induced cell death?
2. Is YAP/TAZ signaling altered by doxorubicin treatment?
3. Does modulation of YAP/TAZ affect cell functions?
4. Does modulation of YAP/TAZ affect doxorubicin-induced cell death?

The second part of this thesis work focuses on the discovery of mechanisms and developmental steps leading to the development DiGeorge syndrome, aiming to answer the following questions:

1. What are the *in vitro* phenotypes where DiGeorge hiPSC lines and their differentiated derivatives show differences as compared to control cells or to each other?

Finally, I present a method for studying calcium signaling in hiPSC-derived neural progenitor cells (hiPSC-NPCs), providing the basis for further studies of the neural aspects of DiGeorge syndrome, aiming to answer the following question:

1. How can intracellular calcium signaling be studied for functional characterization in hiPSC-NPCs not showing spontaneous calcium transients?

3. Results

3.1. Studying YAP/TAZ signaling in hiPSC-CMs for modeling doxorubicin induced cardiotoxicity

YAP is an upstream regulator of differentially expressed genes in human ventricular myocardium samples of patients with doxorubicin-induced heart failure compared to healthy controls based on RNA sequencing analysis [90]. As hiPSC-CMs are suitable for the characterization of molecular mechanisms of cardiotoxicity [77, 126], we generated a human *in vitro* model using hiPSC-CMs to study the role of YAP/TAZ in doxorubicin-induced cardiotoxicity and subsequent cell death.

3.1.1. Doxorubicin induces YAP/TAZ nuclear translocation and cell death

hiPSC-CMs (iCell Cardiomyocytes, Cat. No. 11713, FujiFilm Cellular Dynamics, Inc., Madison, WN, USA) and an estrogen and progesterone receptor-positive human breast cancer cell line MCF7 were used to investigate the effects of chemotherapeutic drugs on cell death. 96 antineoplastic and cardiotherapeutic drugs were tested by using the FDA/EMA-approved Prestwick drug library (Fig. 6. A). High content screening showed that anthracycline agents, such as doxorubicin and daunorubicin, decreased cell viability (as shown by decreased mitochondrial membrane potential) and induced greater nuclear translocation of YAP/TAZ than other classes of drugs in both cell types. High TO-PRO-3 positivity (a marker of necrosis) was observed in response to doxorubicin in breast cancer cells but not in hiPSC-CMs (Fig. 6. A). Further exploring cell death in hiPSC-CMs, we found that hallmarks of apoptosis, such as activation of caspase 3/7, mitochondrial depolarization and nuclear fragmentation [163, 164], were increased in response to doxorubicin exposure in a concentration-dependent manner (Fig. 6. B). However, necrosis was only induced in up to 7 % of hiPSC-CMs in response to 3 µM doxorubicin (Fig. 6. B).
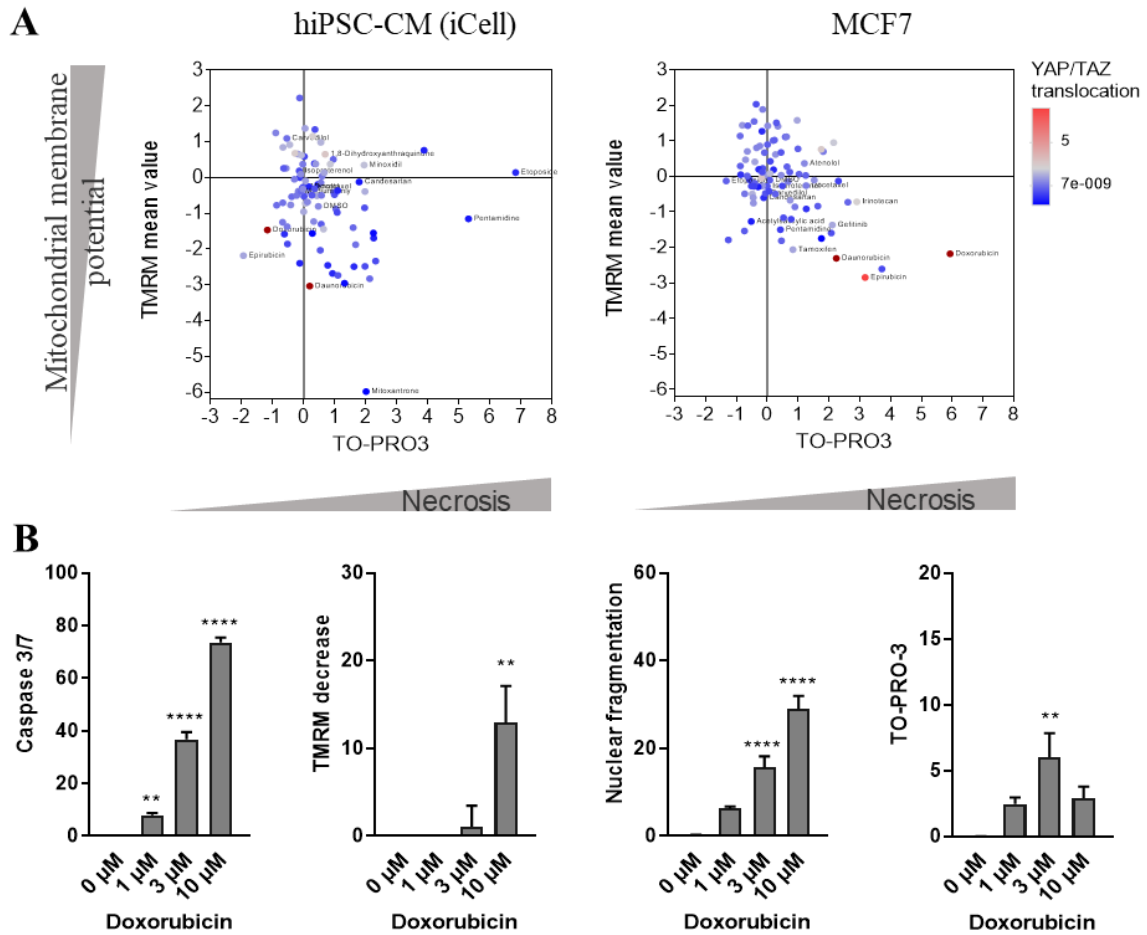
Figure 6. **YAP/TAZ activation and cell death profile of hiPSC-CM after drug treatment** (Image based on [90])

(**A**) YAP/TAZ activation is shown color coded in relation to necrosis as indicated by TO-PRO-3 staining and mitochondrial membrane potential (TMRM) levels in response to antineoplastic and cardiotherapeutic drugs in hiPSC-CMs and MCF7 cancer cells. Each dot represents an individual drug. (**B**) Changes in cell death markers in hiPSC-CM in response to increasing doxorubicin concentrations, percentage of positive cells is shown on the y axis (one-way ANOVA, ** $p < 0.01$, **** $p < 0.0001$, n=3).

3.1.2. Modulating YAP/TAZ expression and activation in hiPSC-CMs affects cell survival in doxorubicin treatment

YAP and TAZ mRNAs were expressed in hiPSC-CMs, as well as in human fetal heart tissue and adult ventricular cardiomyocytes, however, mRNA levels of YAP and TAZ were lower

in *in vitro* differentiated hiPSC-CMs compared to those in human *ex vivo* samples (Fig. 7. A). YAP and TAZ are mechanotransducers, regulated by cell-extracellular matrix contacts and cell-cell contacts [78, 165]. Increases in cell density have been shown to decrease YAP and TAZ activity in other cell populations [166, 167]. To validate our cell culture model, we questioned whether cell density of hiPSC-CMs could affect YAP/TAZ expression and nuclear translocation. We found that YAP and TAZ mRNA levels were decreased in densely plated cells compared to sparsely plated cell populations (Fig. 7. B). YAP/TAZ nuclear translocation was also decreased in dense cultures (Fig. 7. B and C). These results corresponded with the known effects of mechanical cues on YAP and TAZ regulated by cell-cell connections [168].
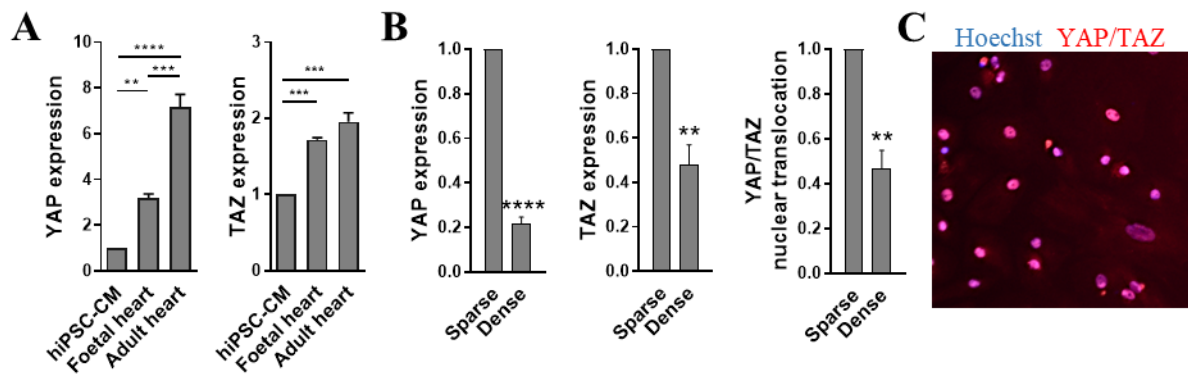

Figure 7. **Expression of YAP/TAZ** (Image based on [90])
(**A**) YAP and TAZ mRNA levels in hiPSC-CMs, fetal and adult heart (one-way ANOVA, ** $p < 0.01$, *** $p < 0.001$, **** $p < 0.0001$, n=3). (**B**) mRNA expression of YAP and TAZ, and YAP/TAZ nuclear translocation in sparse and dense hiPSC-CM cell cultures (paired t-test, ** $p < 0.01$, **** $p < 0.0001$, n=3). (**C**) Immunocytochemistry of YAP/TAZ showing nuclear translocation of YAP/TAZ in control hiPSC-CMs.

Next, we investigated whether modulation of YAP and TAZ expression levels has an effect on cardiomyocyte function and doxorubicin-induced cell death. Transient silencing of both YAP and TAZ by siRNA resulted in a decrease in respective mRNA levels (Fig. 8. A). Transient overexpression of YAP by pEGFP-C3-hYAP1 plasmid nucleofection in hiPSC-CMs (Fig. 8. C) resulted in an over 8000-fold increase in mRNA levels compared to cells transfected with GFP+ plasmid as control (Fig. 8. B). We next investigated whether

YAP/TAZ gene silencing leads to modification of cardiac function by examining calcium transients as a hallmark of cardiomyocyte function using Fura-4F intracellular calcium indicator. Gene silencing did not affect calcium transient amplitude, time to peak or decay (Fig. 8. D). To note, calcium transient analysis with Fura-4F in YAP-overexpressing cells was not possible due to overlapping emission wavelength of Fura-4F and enhanced green fluorescent protein (eGFP).
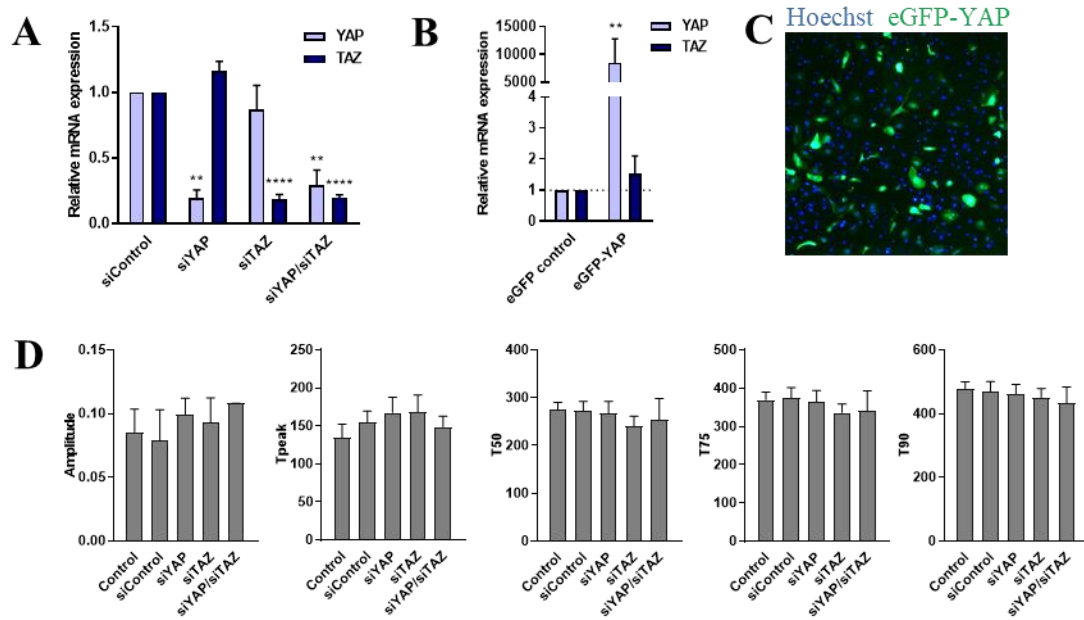

Figure 8. **Altered YAP/TAZ expression does not modulate calcium transient parameters in hiPSC-CMs** (Image based on [90])

(**A**) Silencing of YAP, TAZ or YAP/TAZ together and (**B**) overexpression of YAP in hiPSC-CMs. (**C**) Representative image showing eGFP-YAP expression in eGFP-YAP transfected hiPSC-CMs. (**D**) Calcium transient kinetics in YAP, TAZ or YAP/TAZ silenced hiPSC-CMs. (One-way ANOVA, ** $p<0.01$, **** $p<0.0001$, n=3).

Next, total cell count, necrosis marker TO-PRO-3 and mitochondrial membrane potential marker tetramethylrhodamine, methyl ester (TMRM) intensity were measured to assess the influence of YAP/TAZ modulation (silencing YAP and/or TAZ, or overexpression of YAP) on cell survival in doxorubicin treatment. High concentration of doxorubicin (15 µM) led to a significant decrease in cell number in hiPSC-CMs, and silencing YAP or TAZ, or

YAP/TAZ together did not appear to influence this cellular phenotype (Fig. 9. A). In contrast, YAP overexpression resulted in increased cell number of untreated hiPSC-CMs. It decreased the level of cell loss in response to doxorubicin resulting in comparable total cell count to untreated control cells (Fig. 9. A). We found no significant difference between doxorubicin and vehicle-treated cells when measuring necrosis marker TO-PRO-3 (Fig. 9. B). On the other hand, decrease in mitochondrial membrane potential was more prominent in case of silencing YAP or YAP/TAZ compared to silencing TAZ only or siControl (Fig. 9. C), indicating that loss of YAP may further induce mitochondrial membrane potential loss after doxorubicin treatment. In contrast to eGFP control cells, doxorubicin-induced mitochondrial membrane potential loss remained non-significant in YAP overexpressing hiPSC-CMs (Fig. 9. C).

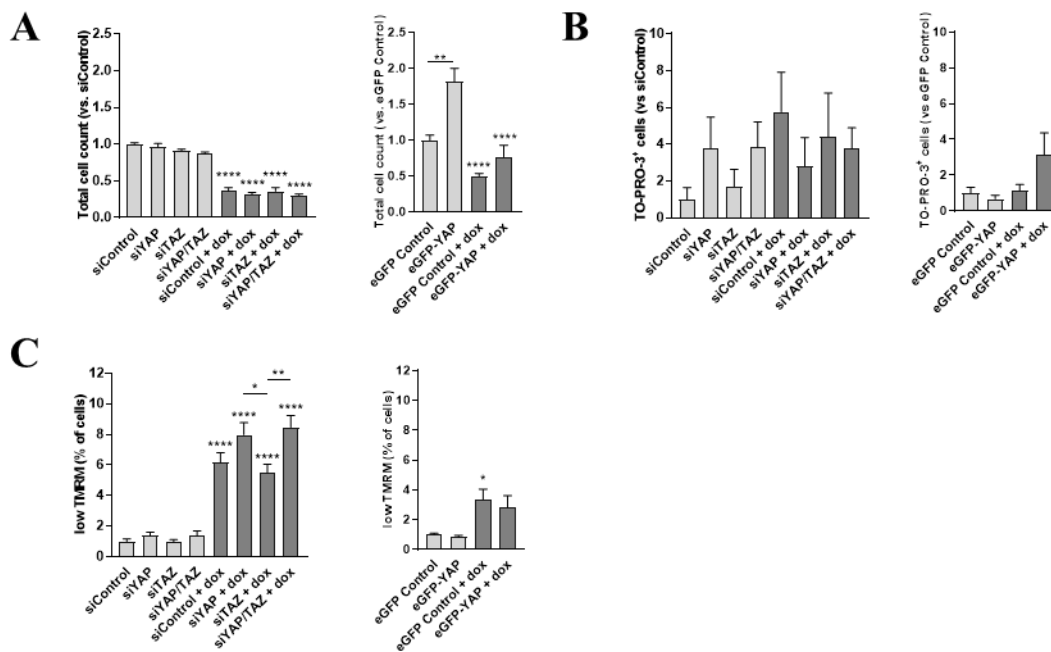Figure 9. **YAP overexpression induces proliferation and inhibits doxorubicin-induced apoptosis hiPSC-CMs** (Image based on [90])

(**A**) Bar charts showing the effects of YAP, TAZ, or YAP/TAZ silencing or YAP-overexpression on cell number, (**B**) necrosis and (**C**) mitochondrial membrane potential in hiPSC-CMs in response to doxorubicin treatment.

(One-way ANOVA, * $p<0.05$, ** $p<0.01$, **** $p<0.0001$, n=3).

3.2. Modeling the cardiovascular features of DiGeorge syndrome

3.2.1. Clinical description of human subjects involved in this study

A family with three DiGeorge patients from three generations (grandfather, mother and child) manifesting the disease with different severity, and two healthy relatives were involved in this study (Fig. 10., Supplementary material). Mild symptoms of the grandfather consist of articulation disorder and minimal facial dysmorphia. Moderate symptoms of the mother include vascular ring (surgically corrected in childhood), hypocalcemia and minimal facial dysmorphia. Symptoms of the child were severe and led to death at the age of 5 months; tetralogy of Fallot (ventricular septal defect, pulmonary atresia, right ventricular hypertrophy, misplaced aorta), atrial septal defect, asymmetric brain ventricles, hypocalcemia, hypoparathyroidism and minimal facial dysmorphia. The cause of death was cerebral herniation (shifting of cerebral tissue from its normal location into an adjacent space [169]).
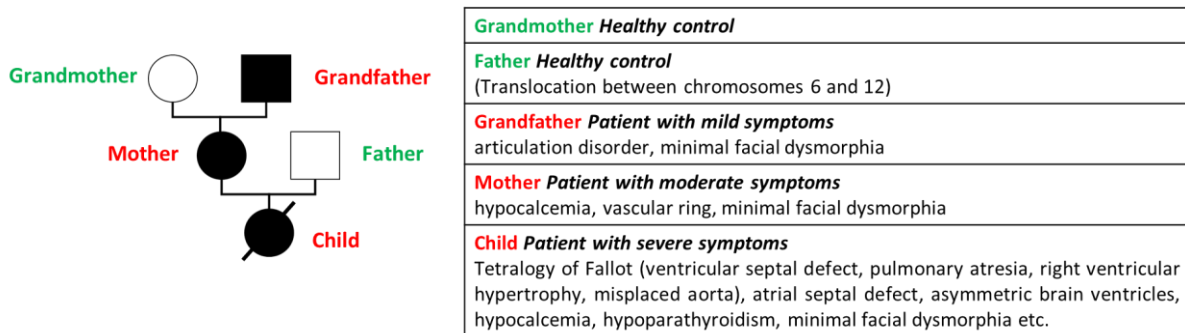
Figure 10. **Pedigree of the family involved in the study**

Clinical symptoms of patients show increasing severity when the disease is inherited.

Karyotype testing of peripheral blood mononuclear cells (PBMCs) revealed chromosomal translocation between chromosomes 6 and 12 in the father. However, balanced translocations of this kind, when breakpoints are not in gene sequences or regulatory elements, usually do not cause phenotypic changes [170]. The translocation was not inherited to the child. Considering that the father is a healthy individual, the breakpoint details were not further characterized.

3.2.2. Generation and characterization of hiPSC lines

Reprogramming of PBMCs isolated from blood samples of all family members was performed by Sendai virus transduction [161]. Pluripotency was verified by expression of pluripotency markers OCT4, NANOG and stage-specific embryonic antigen 4 (SSEA-4) (data not show).

Karyotype testing showed no chromosomal alterations in hiPSC lines, with the exemption of the translocation between chromosomes 6 and 12 in hiPSCs of the father, later showed to be present in PBMCs, proving that it was not generated during reprogramming.

The typical 3 Mb long deletion of the 22q11.2 region was verified by multiplex ligation-dependent probe amplification (MLPA) genetic test in hiPSC lines of all the three DiGeorge patients (data not show).

3.2.3. Cardiac differentiation and characterization of cardiomyocytes

hiPSCs were differentiated into cardiomyocytes based on a previously described protocol [171]. Immunostaining with the cardiac-specific marker troponin I3, cardiac type (TNNI3) showed high purity of cardiomyocytes in the cell culture on day 36 of differentiation (>95%) (Fig. 11. A). This was further confirmed by mRNA expression analysis of multiple cardiac differentiation markers, with no difference between cell lines (Fig. 11. B.). The used differentiation protocol yields in a mixed population of cardiac subtypes, and cells thus express ventricular (myosin light chain 2 (MYL2)), atrial (myosin light chain 7 (MYL7)) and pacemaker (hyperpolarization activated cyclic nucleotide gated potassium channel 4 (HCN4)) markers [172].

Cardiac gap junction proteins (connexins) have been implicated to have a role in the development of cardiac anomalies, including TOF [173]. Cx40 (gap junction protein alpha 5 (GJA5)) and Cx43 (gap junction protein alpha 1 (GJA1)) are two major gap junction proteins in the heart. Measurement of the expression of these two genes in cardiomyocytes showed a significantly lower level of GJA1 in the child's cells. In contrast, there was no difference observed in the expression of GJA5 (Fig. 11. C).

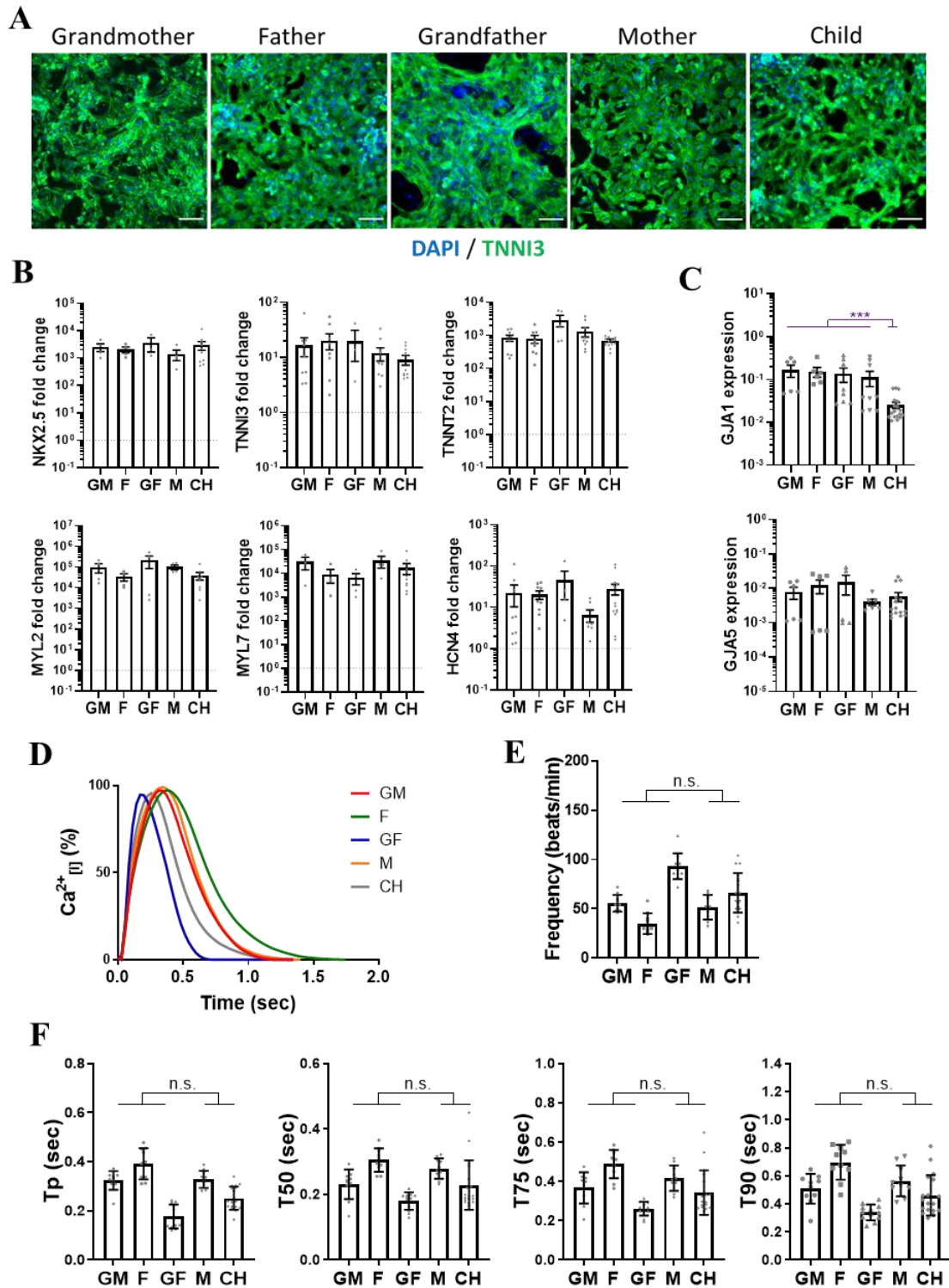Figure 11. **Characterization of hiPSC-derived cardiomyocytes**

(**A**) Immunostaining for cardiac marker TNNI3 on day 36 (scale bar: 100 mm). (**B**) mRNA

expression measurements of cardiac differentiation markers on day 36, fold change compared

to expression in respective hiPSCs (one-way ANOVA, non-significant, n=3). (**C**) mRNA levels of cardiac connexins and DiGeorge associated genes (unpaired t-test, *** p<0.001, n=3). (**D**) Intracellular calcium changes (mean values are shown for each cell line) and (**E**) frequency analysis on day 36 of cardiac differentiation. (**F**) Analysis of calcium kinetic parameters (Tp: time to peak, T50: 50 % decay, T75: 75 % decay, T90: 90 % decay). (Unpaired t-test, n.s. – non significant, n=3).

(GM: grandmother, F: father, GF: grandfather, M: mother, CH: child).

For functional characterization, analysis of intracellular calcium signals allows us to study calcium transient kinetics, depending on beating frequency. (Fig. 11. A-C). To test if *in vitro* phenotypes of cardiomyocyte function can be associated with patients with cardiovascular symptoms, hiPSC-CMs of mother and child were compared to the group of individuals without cardiovascular symptoms (controls and grandfather). No significant differences in frequency and calcium transient kinetics were observed in this case, suggesting that altered cardiomyocyte function is not the cause of cardiovascular symptoms in DiGeorge syndrome (Fig. 11. A-C).

3.2.4. Neural crest differentiation and characterization of neural crest spheroids and migratory neural crest cells

Most results presented in this chapter are preliminary, but principally show our approaches in the search for *in vitro* phenotypes. hiPSCs were differentiated into neural crest cells based on a previously described protocol [68]. All cell lines produced migratory neural crest cells, however, immunostainings of neural crest markers SRY-box transcription factor 9 (SOX9) and AP2α (transcription factor AP-2 alpha (TFAP2A)) showed significantly decreased intensity levels in NCCs of DiGeorge cell lines compared to controls (Fig. 12. A and B). Consistent with immunostaining results, mRNA expression levels of SOX9 and AP2α were decreased in DiGeorge cell lines compared to controls. Additionally, expression levels of another neural crest marker P75 (nerve growth factor receptor (NGFR)) in DiGeorge cells were also decreased compared to controls (Fig. 12. C). These results thus show that low expression of multiple neural crest markers is a characteristic of NCCs of DiGeorge patients and indicate a defective capacity to reach and maintain a proper specified neural crest state.
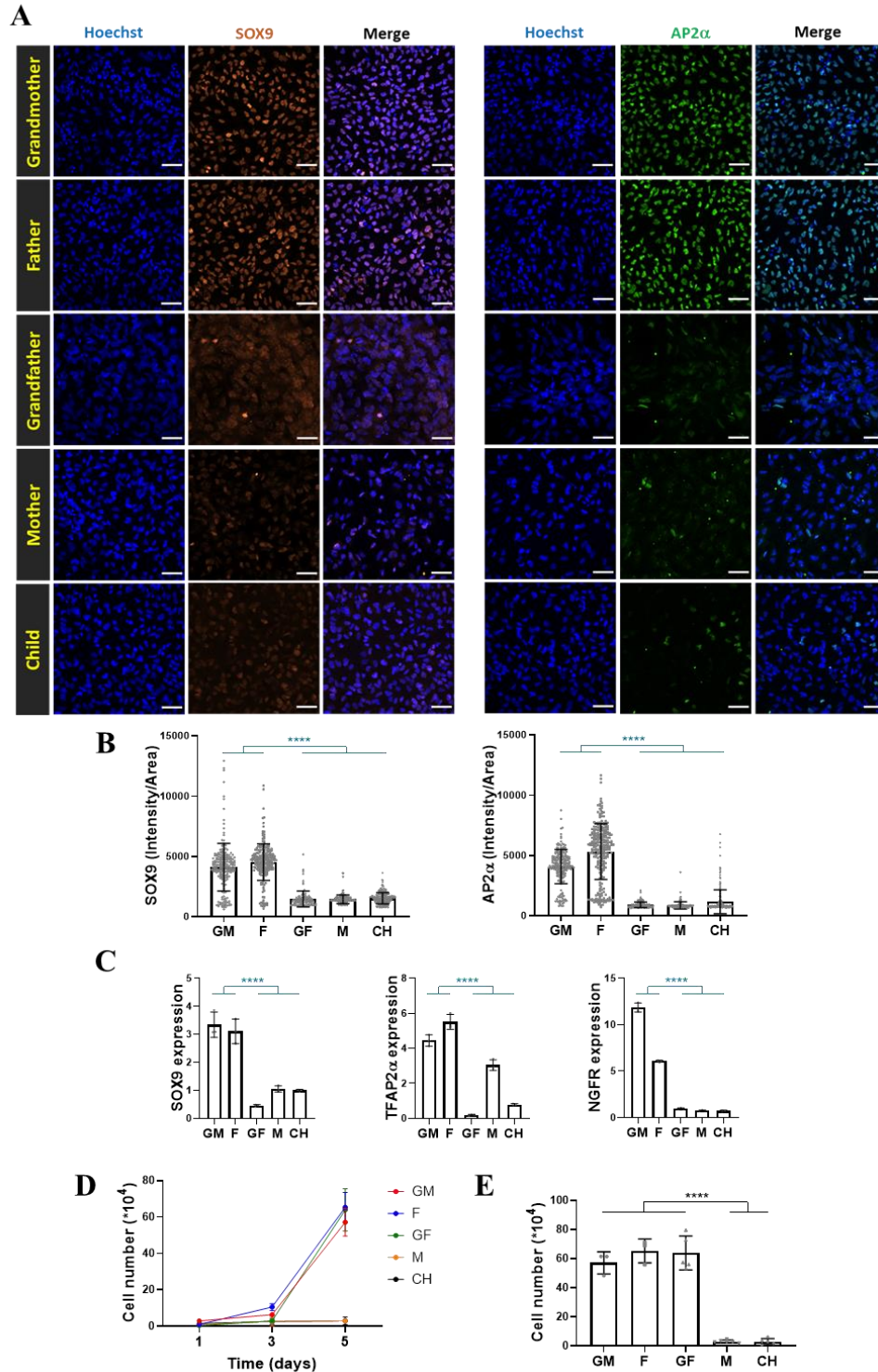
Figure 12. **Characterization of migratory neural crest cells**

(**A**) Immunostainings for SOX9 and AP2α neural crest markers on migratory neural crest cells at passage 1 (scale bar: 50 mm). (**B**) Analysis of SOX9 and AP2α intensities in

individual cells normalized to the size of nuclei. (**C**) mRNA expression measurements of neural crest markers on migratory neural crest cells at passage 1. (Unpaired t-test, **** $p<0.0001$, n=1). (**D**) Growth curve of passage 2 neural crest cells. (**E**) Analysis of viable cell number on day 5 after passaging (unpaired t-test, **** $p<0.0001$, n=3).

(GM: grandmother, F: father, GF: grandfather, M: mother, CH: child).

Next, we asked whether NCC function was changed in the migrating NCCs derived from DiGeorge syndrome patient cells. For this, we addressed cell growth. Growth curve based on viable cell counting showed a significantly decrease in cell number of hiPSC-NCCs of the mother and child compared to controls and grandfather (Fig. 12. D and E). Interestingly, the viable cell number of the grandfather was at the level of the controls with an obvious difference compared to the mother and child. The results show that hiPSC-NCC viability was affected in cells of DiGeorge patients with cardiovascular symptoms (mother and child) but was not altered in the cells of DiGeorge patient with no cardiovascular symptoms (grandfather). If this happens by cell death or decreased proliferation rate is under investigation.

3.3. Studying calcium signaling in hiPSC-derived hippocampal DG NPCs

Previous *in vitro* models for 22q11.2DS show that calcium handling is affected in neuronal differentiation of patient-derived hiPSCs [96]. However, there has been no human-based report studying calcium signaling in hippocampal dentate gyrus granule cells in DiGeorge syndrome. For this aim, we developed techniques for studying calcium signaling in hiPSC-derived hippocampal NPCs and DG granule cells comparing a cytoplasmic Ca^{2+} dye; Fluo-4 and a genetically encoded Ca^{2+} indicator; GCaMP6 [162]. In this chapter, I representatively show our experiments with Fluo-4, being more suitable for our future experiments.

3.3.1. Ligand-induced calcium signaling in hippocampal NPCs

As expected, neural progenitor cells did not show significant spontaneous calcium transients. For the investigation of their calcium homeostasis ATP, lysophosphatidic acid (LPA) and trypsin were applied as ligands to trigger calcium signals in the cells. Ionomycin Ca^{2+} ionophore was applied to release Ca^{2+} from intracellular stores. The intracellular calcium signal intensity triggered by ionomycin was set as the maximum Ca^{2+} content of the cells and ethylene glycol-bis(β-aminoethyl ether)-N,N,N′,N′-tetraacetic acid (EGTA) calcium chelator was applied to set the background (calcium-independent fluorescence) in our experiments. Approximately 12 % of the cells showed calcium response to ATP (Fig. 13. A) and nearly all the cells responded to trypsin (Fig. 13. B). The effect of these ligands was blocked when specific inhibitors were applied. Approximately 20 % of the cells showed calcium oscillations following ATP, LPA and trypsin treatment (Fig. 13. C), indicating the transmission of intracellular biological information [174].
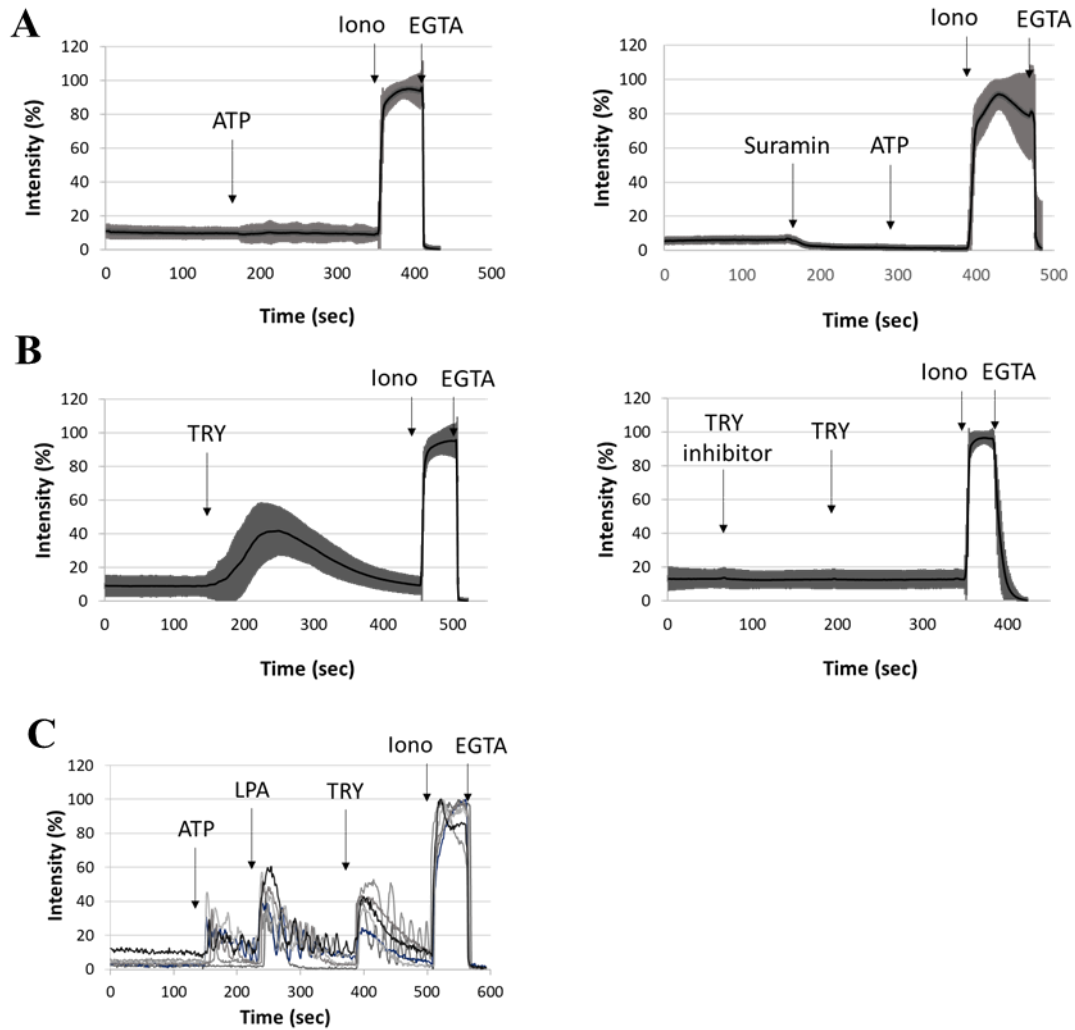
Figure 13. **Calcium signals evoked by ligands in hiPSC-derived hippocampal NPCs** (Image based on [162])

(**A**) Calcium signals triggered by ATP are blocked by suramin P2 purinergic receptor inhibitor and (**B**) calcium signals triggered by trypsin are blocked by trypsin inhibitor in hiPSC-NPCs (Mean±SEM). (**C**) Calcium oscillations triggered by ATP, LPA and trypsin in individual hiPSC-NPCs.

The number of responding NPCs to glutamate neurotransmitter was highly variable between 20 to 80 % with relatively low signal intensity (Fig. 14. A) and hiPSC-NPCs did not show depolarization in response to potassium chloride (KCl) membrane depolarizing agent, proving the undifferentiated progenitor state of these cells. Finally, hiPSC-NPCs were further differentiated into neurons to test their differentiation capacity. In excitatory neurons, an

action potential is followed by a calcium transient due to calcium influx [175]. We tracked the emergence of spontaneous, rhythmic calcium activity after changing culture conditions and shifting NPCs from proliferation to differentiation and all the cells responded to glutamate neurotransmitter (Fig. 14. B), showing the differentiation capacity of the NPCs into glutamatergic neurons.
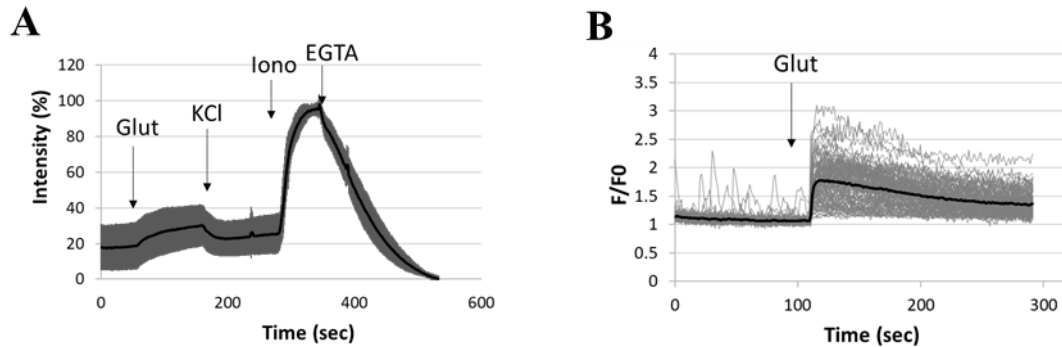

Figure 14. **Calcium signals in hiPSC-derived hippocampal NPCs and neurons** (Image based on [162])

(**A**) Calcium signals in response to glutamate (Glut) and KCl in hiPSC-NPCs (Mean±SEM). (**B**) hiPSC-derived hippocampal DG neurons show spontaneous calcium transients and calcium response to glutamate.

4. Discussion

Cardiovascular diseases are the first, and neurological diseases are the second leading cause of death worldwide [1, 2], strongly motivating researchers to study the cause and mechanisms leading to the development of these diseases. Patient-specific hiPSC lines are suitable for disease modeling, particularly in human cell types which cannot be investigated directly or in the long-term, or when appropriate animal models are not available. In this thesis, I show examples for how to use hiPSC-derivatives for disease modeling.

The first model aimed to investigate Hippo pathway-YAP/TAZ signaling in doxorubicin induced cardiotoxicity, as an example for modeling drug-induced disease.

Traditional chemotherapeutic drug families, like anthracyclines, are highly effective drugs in several cancer types [72, 73], however, these drugs can cause cardiac dysfunction leading to a high risk of developing heart failure in cancer survivors [73]. Yet our current knowledge of the underlying mechanisms is limited. Hippo pathway-YAP/TAZ signaling has been identified in various types of cancer controlling growth and as a tumor suppressor pathway [176, 177]. Based on our RNA-sequencing analysis of left ventricular samples from cancer patients with doxorubicin-induced heart failure and healthy controls, we previously found that YAP is one of the top upstream regulators of differentially expressed genes, indicating that YAP may have a role in doxorubicin-induced cardiotoxicity [90].

To confirm this, we generated an *in vitro* model using hiPSC-CMs to investigate the role of YAP/TAZ in doxorubicin-induced cell death. Testing a library of 96 antineoplastic and cardiotherapeutic drugs, doxorubicin was the strongest inducer of YAP/TAZ nuclear translocation in both breast cancer cells and hiPSC-CMs. Cancer cells and hiPSC-CMs presented different cell death profiles in response to doxorubicin. Doxorubicin primarily induced necrosis in breast cancer cells, whereas hiPSC-CMs showed induction of apoptosis but not necrosis. Doxorubicin led to elevated levels of caspase 3/7, nuclear fragmentation, and a decrease in mitochondrial membrane potential in a concentration-dependent manner in hiPSC-CMs, indicating that doxorubicin-induced toxicity occurs primarily through apoptosis. Doxorubicin also induced YAP/TAZ activation in hiPSC-CMs, measured as YAP/TAZ nuclear translocation. Cell density proved to be a factor regulating YAP/TAZ activation; increase in YAP and TAZ mRNA expression and YAP/TAZ activation was

observed in sparse hiPSC-CMs as compared with dense cell cultures. Therefore, it is not clear if doxorubicin induces YAP/TAZ activation directly, or as a consequence of doxorubicin-induced cell loss and subsequent lower cell density, corresponding with the mechanotransducer role of YAP/TAZ activated by altered extracellular and cell-cell connections [85, 89]. Transient silencing of YAP and TAZ co-activators resulted in a modest mitochondrial membrane potential loss in hiPSC-CMs. Contrarily, overexpression of YAP improved doxorubicin-induced cell death markers such as reduction in mitochondrial membrane potential and cell loss by increasing cell proliferation. These results suggest that increasing YAP expression may be a beneficial strategy against doxorubicin-induced cardiotoxicity. Given that increased YAP expression might lead to drug resistance in cancer cells [178, 179], it is important to consider cardio-selective YAP activation when developing new cardioprotective strategies [177, 180, 181].

The second model in this thesis work focused on studying DiGeorge syndrome, as an example for modeling a complex genetic disease.

DiGeorge syndrome is the most common microdeletion syndrome [92], caused by a monoallelic deletion of 22q11.2 chromosome region. Close to two-third of DiGeorge patients develop CHD delays [92] and more than 30% suffer from psychiatric symptoms [95, 96]. Severity of symptoms usually increases when the disease is inherited [97]. Here we generated the first hiPSC lines for an inherited form of DiGeorge syndrome from three generations. Patients in our study showed the typical 3 Mb deletion of the 22q11.2 chromosome region, but manifest the disease with different severity.

Functional cardiomyocytes could be differentiated from all DiGeorge and control cell lines expressing multiple cardiac differentiation markers. Calcium signal analysis failed to show significant differences between individuals with (mother and child) and without (controls and grandfather) cardiovascular symptoms. Interestingly, we found a significantly decreased mRNA level of Cx43 (GJA1) in cardiomyocytes of the child. Gap junction protein Cx43 is the main cardiac gap junction protein [182] and disturbances of Cx43 levels have been shown to contribute to TOF development [173, 183]. Taken together, our results implicate that cardiac malformations, such as TOF in DiGeorge syndrome, might originate from cell-cell connections in the heart, rather than altered cardiomyocyte function.

cNCCs are essential components of normal cardiovascular development [51]. Loss or dysregulation of cNCCs can lead to CHDs and has been indicated to be associated with cardiovascular symptoms in DiGeorge syndrome [50, 51]. Migratory NCCs could be differentiated from all the cell lines in our study, although decreased levels of SOX9, AP2α and P75 NC markers were observed in cells of DiGeorge patients compared to controls. These markers are responsible for NC specification [184, 185], delamination [186-188], and later NC development [189]. These results indicate a defect to reach and maintain a proper specified neural crest state in DiGeorge syndrome. Cell growth analysis of migratory NCCs showed significantly decreased cell number in case of the mother and child as compared to controls and grandfather. Whether this is caused by apoptosis and/or lower proliferation rate, is under investigation. Our results indicate that decreased NC cell number is a characteristic of DiGeorge patients with increased overall severity of symptoms, including the cardiovascular defects.

Functional deficit of hippocampal NPCs can be an implication for psychiatric disorders [190]. Detailed study of calcium homeostasis and calcium transient kinetics in hiPSC-derived hippocampal NPCs and DG granule cells makes it possible to investigate specific neuronal differentiation steps and functionality in disease models. Calcium deficit has been shown in hiPSC-cortical neurons of 22q11.2DS patients [96] and altered gene expression and function of hippocampal dentate granule neurons in 22q11.2DS has been shown in mouse models [110, 111]. We have established an *in vitro* modeling system for studying calcium signaling in hiPSC-derived hippocampal NPCs, and we are planning the first hiPSC-based study for the functional characterization of this cell type in DiGeorge syndrome. hiPSC-derived hippocampal NPCs did not show spontaneous calcium transients and were not depolarized by KCl, showing the undifferentiated progenitor state. Application of ligands triggering calcium signals is needed to study calcium signaling for functional analysis of these cells. ATP, LPA and trypsin proved to be adequate ligands for this aim, and with a specific calibration method, the triggered signal intensity and the ratio of responding cells in the cell culture can be assessed. As hippocampal granule cells are glutamatergic neurons in the DG [155, 156], we tested whether hiPSC-NPCs are responsive to glutamate. Interestingly, a highly variable number of responding cells was observed in hiPSC-NPC cultures showing

relatively low signal intensity. When these cells were further differentiated into neurons, all the cells were observed to be responsive to glutamate neurotransmitter, proving the capacity of hiPSC-NPCs to differentiate into glutamatergic neurons. In summary, these results show that our method is suitable for functional characterization of hiPSC-NPCs and neurons and will be applied to study plasticity and disease related phenotypes in these cell types.

Future perspectives of this project also include RNA sequencing analysis of hiPSC lines and differentiated derivatives at multiple stages to further elucidate the expression pattern changes in disease, and to identify novel candidate genes and signaling pathways associated with the specific symptoms in DiGeorge syndrome. Previously performed comparative genomic hybridization (CGH) and whole-exome sequencing (WES) data from the hiPSC lines (data not shown) will be combined with the RNA sequencing data as well, to investigate the contribution of copy number variations and genetic variants in addition to the 22q11.2 deletion, and how the genetic characteristics alter the transcriptional profile.

In conclusion, in this thesis work I show that hiPSC-based *in vitro* disease modeling systems provide the possibility to study disease mechanisms in cardiotoxicity and complex diseases.

5. Conclusions

The aim of this thesis work is to generate hiPSC-based *in vitro* models for better understanding cellular and molecular level disease mechanisms aiming to help the development of preventive strategies and treatment.

In the first model presented, the role of YAP/TAZ in doxorubicin-induced cardiotoxicity was investigated. We found that out of the tested 96 antineoplastic and cardiotherapeutic drugs, doxorubicin was the strongest inducer of YAP/TAZ nuclear translocation in both breast cancer cells and hiPSC-CMs, indicating that doxorubicin activates YAP/TAZ signaling. Doxorubicin-induced cell death was mediated by apoptosis, but not by necrosis in hiPSC-CMs. On the other hand, necrosis was induced in breast cancer cells as a result of doxorubicin treatment. YAP/TAZ expression and activation was decreased by increased cell density, corresponding with the mechanotransducer role of YAP/TAZ regulated by cell-ECM and cell–cell connections [85, 89]. Silencing YAP/TAZ did not alter calcium transients in hiPSC-CMs, indicating that YAP/TAZ does not regulate cardiomyocyte function. Overexpression of YAP rescued doxorubicin-induced cell loss by inhibiting apoptosis and through induction of proliferation in hiPSC-CMs. Based on our results, we conclude that cardio-selective increase of YAP expression could be a cardioprotective strategy during doxorubicin treatment of cancer patients.

In the second model, patient-derived hiPSCs were differentiated into relevant cell types to model the cardiovascular aspects of DiGeorge syndrome. We generated for the first time hiPSC lines for an inherited form of DiGeorge syndrome from three generations manifesting the disease with different severity with the typical 3 Mb deletion of the 22q11.2 chromosome region. We did not experience differences in expression of multiple cardiac differentiation markers and calcium transient analysis of hiPSC-CMs comparing patients with (mother and child) and without cardiovascular symptom (controls and grandfather. Cx43 (GJA1), a major gap junction protein in the heart showed significantly lower expression in hiPSC-CMs of the child. Based on these results we conclude that cardiomyocyte differentiation *per se* is not

affected in DiGeorge syndrome, but structural development and molecular expression patterns in the heart can be involved in the mechanisms driving cardiovascular symptoms.

All cell lines were able to produce migratory NCCs, although decreased expression of multiple neural crest markers in cells of DiGeorge patients was observed allowing us to conclude that NCCs in DiGeorge syndrome are not able to develop normally. Additionally, impaired cell growth was observed in NCCs from DiGeorge patients with cardiovascular symptoms (mother and child). This indicates that decreased expression of neural crest markers combined with compromised cell growth of NCCs can be a factor leading to cardiovascular anomalies in DiGeorge syndrome.

Neurological disorders are frequent among DiGeorge patients with 30 % developing schizophrenia and 30-40 % developing autism spectrum disorder [95, 96]. Calcium deficit has been shown in cortical neurons differentiated from hiPSCs of 22q11.2DS patients [96]. However, there has been no hiPSC-based study investigating hippocampal DG granule cells in patients with 22q11.2 deletion, despite that this region has been associated with many neurological conditions including schizophrenia and the involvement of these cells in 22q11.2DS has been shown in mice [110, 111]. To this aim, we have established an *in vitro* modeling system for studying calcium signaling in hiPSC-derived hippocampal NPCs [162], suitable to study NPC plasticity and potential disease related phenotypes. ATP, LPA and trypsin proved to be suitable for triggering calcium signals in hiPSC-NPCsand with a specific calibration method, characteristics of the triggered signal could be assessed. In our further experiments DiGeorge patient-derived and control cell lines will be studied accordingly.

Additionally, ongoing RNA sequencing analysis of hiPSC lines and derivatives at multiple differentiation stages combined with CGH and WES data from the hiPSC lines aims to unfold the molecular and genetic background of *in vitro* phenotypes, giving us a basis for the association with the clinical manifestations.

Main findings:

Studying YAP/TAZ signaling in doxorubicin induced cardiotoxicity using hiPSC-CMs

- Doxorubicin-induced cell death was mediated by apoptosis, but not by necrosis in hiPSC-CMs.

- Out of the tested 96 antineoplastic and cardiotherapeutic drugs, doxorubicin was the strongest inducer of YAP/TAZ nuclear translocation in both breast cancer cells and hiPSC-CMs, indicating that doxorubicin activates YAP/TAZ signaling.

- Silencing YAP/TAZ did not alter calcium transients in hiPSC-CMs, indicating that YAP/TAZ does not regulate cardiomyocyte function.

- Silencing of YAP and TAZ co-activators resulted in a modest mitochondrial membrane potential loss in hiPSC-CMs. Contrarily, overexpression of YAP rescued doxorubicin-induced cell loss by inhibiting apoptosis and through induction of proliferation in hiPSC-CMs.

- We conclude that cardio-selective increase of YAP expression could be a cardioprotective strategy during doxorubicin treatment of cancer patients.

Modeling DiGeorge syndrome with hiPSC-derivatives

- Cardiac differentiation was not affected in DiGeorge syndrome, but molecular expression patterns could show differences.

- Defects in proper NCCs differentiation was a characteristic of DiGeorge syndrome and combined with decreased cell viability could be a factor contributing to the cardiovascular symptoms.

Studying calcium signaling in hiPSC-derived hippocampal NPCs

- In the established *in vitro* modeling system for studying calcium signaling in hiPSC-derived hippocampal NPCs we found that ATP, LPA and trypsin are suitable for triggering calcium signals in hiPSC-NPCs.

- Characteristics of the triggered signal can be assessed using a specific calibration method.

- We conclude that this system is suitable to study NPC plasticity and potential disease related phenotypes.

6. Summary

This thesis focuses on how to use hiPSC-derivatives in disease modeling to discover the underlying mechanisms and to potentially develop strategies for prevention and treatment.

In the first model presented in this thesis, the role of YAP/TAZ in doxorubicin-induced cardiotoxicity was investigated. Our results showed that doxorubicin-induced cardiac death is mediated primarily by apoptosis and not necrosis. YAP/TAZ is activated in response to doxorubicin treatment, suggesting that the YAP/TAZ signaling plays a role in doxorubicin-induced cardiotoxicity. Silencing YAP/TAZ did not alter calcium transients in hiPSC-CMs, indicating that YAP/TAZ does not regulate cardiomyocyte function. Overexpression of YAP rescued doxorubicin-induced cell loss by inhibiting apoptosis and inducing proliferation. Our data add novel insights into the mechanisms of doxorubicin-induced cell loss and suggest a potential cardioprotective effect of YAP in doxorubicin-induced cardiotoxicity.

The second model focuses on modeling DiGeorge syndrome. We generated the first hiPSC lines for an inherited form of DiGeorge syndrome with increasing severity throughout generations and two healthy controls. Functionally active cardiomyocytes were successfully generated from all cell lines and calcium transient analysis and expression of cardiac differentiation markers showed no differentiation or functional deficit in hiPSC-CMs in DiGeorge syndrome, but molecular expression patterns of gap junction proteins can be involved in the cardiovascular symptoms. We further found that neural crest specification is affected in DiGeorge patients based on decreased expression of multiple neural crest markers in migratory NCCs. Finally, cell growth was affected only in NCCs derived from patients with cardiovascular symptoms and may be a factor leading to the increasing severity of the symptoms and cardiovascular anomalies in DiGeorge syndrome.

Additionally, we established an *in vitro* modeling system for studying calcium signaling in hiPSC-derived hippocampal NPCs suitable to study potential disease related phenotypes and we are planning the first hiPSC-based study for the functional characterization of hippocampal DG granule cells in DiGeorge syndrome.

7. References

1. Wu C, Zhang Z, Zhang W, Liu X. (2022) Mitochondrial dysfunction and mitochondrial therapies in heart failure. Pharmacol Res, 175: 106038.

2. Avan A, Hachinski V. (2021) Stroke and dementia, leading causes of neurological disability and death, potential for prevention. Alzheimers Dement, 17(6): 1072-1076.

3. Sunchu B, Cabernard C. (2020) Principles and mechanisms of asymmetric cell division. Development, 147(13).

4. Morrison SJ, Kimble J. (2006) Asymmetric and symmetric stem-cell divisions in development and cancer. Nature, 441(7097): 1068-1074.

5. Choumerianou DM, Dimitriou H, Kalmanti M. (2008) Stem cells: promises versus limitations. Tissue Eng Part B Rev, 14(1): 53-60.

6. Romito A, Cobellis G. (2016) Pluripotent Stem Cells: Current Understanding and Future Directions. Stem Cells Int, 2016: 9451492.

7. Clevers H, Watt FM. (2018) Defining Adult Stem Cells by Function, not by Phenotype. Annu Rev Biochem, 87: 1015-1027.

8. Aboul-Soud MAM, Alzahrani AJ, Mahmoud A. (2021) Induced Pluripotent Stem Cells (iPSCs)-Roles in Regenerative Therapies, Disease Modelling and Drug Screening. Cells, 10(9).

9. Apati A, Varga N, Berecz T, Erdei Z, Homolya L, Sarkadi B. (2019) Application of human pluripotent stem cells and pluripotent stem cell-derived cellular models for assessing drug toxicity. Expert Opin Drug Metab Toxicol, 15(1): 61-75.

10. Takahashi K, Yamanaka S. (2006) Induction of pluripotent stem cells from mouse embryonic and adult fibroblast cultures by defined factors. Cell, 126(4): 663-676.

11. Takahashi K, Tanabe K, Ohnuki M, Narita M, Ichisaka T, Tomoda K, Yamanaka S. (2007) Induction of pluripotent stem cells from adult human fibroblasts by defined factors. Cell, 131(5): 861-872.

12. Yu J, Vodyanik MA, Smuga-Otto K, Antosiewicz-Bourget J, Frane JL, Tian S, Nie J, Jonsdottir GA, Ruotti V, Stewart R, Slukvin, II, Thomson JA. (2007) Induced pluripotent stem cell lines derived from human somatic cells. Science, 318(5858): 1917-1920.

13.   Yu J, Hu K, Smuga-Otto K, Tian S, Stewart R, Slukvin, II, Thomson JA. (2009) Human induced pluripotent stem cells free of vector and transgene sequences. Science, 324(5928): 797-801.

14.   Raab S, Klingenstein M, Liebau S, Linta L. (2014) A Comparative View on Human Somatic Cell Sources for iPSC Generation. Stem Cells Int, 2014: 768391.

15.   Shao L, Wu WS. (2010) Gene-delivery systems for iPS cell generation. Expert Opin Biol Ther, 10(2): 231-242.

16.   Malik N, Rao MS. (2013) A review of the methods for human iPSC derivation. Methods Mol Biol, 997: 23-33.

17.   Chang CW, Lai YS, Pawlik KM, Liu K, Sun CW, Li C, Schoeb TR, Townes TM. (2009) Polycistronic lentiviral vector for "hit and run" reprogramming of adult skin fibroblasts to induced pluripotent stem cells. Stem Cells, 27(5): 1042-1049.

18.   Woltjen K, Michael IP, Mohseni P, Desai R, Mileikovsky M, Hamalainen R, Cowling R, Wang W, Liu P, Gertsenstein M, Kaji K, Sung HK, Nagy A. (2009) piggyBac transposition reprograms fibroblasts to induced pluripotent stem cells. Nature, 458(7239): 766-770.

19.   Zhou W, Freed CR. (2009) Adenoviral gene delivery can reprogram human fibroblasts to induced pluripotent stem cells. Stem Cells, 27(11): 2667-2674.

20.   Ye H, Wang Q. (2018) Efficient Generation of Non-Integration and Feeder-Free Induced Pluripotent Stem Cells from Human Peripheral Blood Cells by Sendai Virus. Cell Physiol Biochem, 50(4): 1318-1331.

21.   Wang AYL. (2021) Application of Modified mRNA in Somatic Reprogramming to Pluripotency and Directed Conversion of Cell Fate. Int J Mol Sci, 22(15).

22.   Warren L, Manos PD, Ahfeldt T, Loh YH, Li H, Lau F, Ebina W, Mandal PK, Smith ZD, Meissner A, Daley GQ, Brack AS, Collins JJ, Cowan C, Schlaeger TM, Rossi DJ. (2010) Highly efficient reprogramming to pluripotency and directed differentiation of human cells with synthetic modified mRNA. Cell Stem Cell, 7(5): 618-630.

23.   Zhou H, Wu S, Joo JY, Zhu S, Han DW, Lin T, Trauger S, Bien G, Yao S, Zhu Y, Siuzdak G, Scholer HR, Duan L, Ding S. (2009) Generation of induced pluripotent stem cells using recombinant proteins. Cell Stem Cell, 4(5): 381-384.

24.   Cieslar-Pobuda A, Knoflach V, Ringh MV, Stark J, Likus W, Siemianowicz K, Ghavami S, Hudecki A, Green JL, Los MJ. (2017) Transdifferentiation and reprogramming: Overview of the processes, their similarities and differences. Biochim Biophys Acta Mol Cell Res, 1864(7): 1359-1369.

25.   Avior Y, Sagi I, Benvenisty N. (2016) Pluripotent stem cells in disease modelling and drug discovery. Nat Rev Mol Cell Biol, 17(3): 170-182.

26.   Rowe RG, Daley GQ. (2019) Induced pluripotent stem cells in disease modelling and drug discovery. Nat Rev Genet, 20(7): 377-388.

27.   Li H, Yang Y, Hong W, Huang M, Wu M, Zhao X. (2020) Applications of genome editing technology in the targeted therapy of human diseases: mechanisms, advances and prospects. Signal Transduct Target Ther, 5(1): 1.

28.   Grobarczyk B, Franco B, Hanon K, Malgrange B. (2015) Generation of Isogenic Human iPS Cell Line Precisely Corrected by Genome Editing Using the CRISPR/Cas9 System. Stem Cell Rev Rep, 11(5): 774-787.

29.   Litvinukova M, Talavera-Lopez C, Maatz H, Reichart D, Worth CL, Lindberg EL, Kanda M, Polanski K, Heinig M, Lee M, Nadelmann ER, Roberts K, Tuck L, Fasouli ES, DeLaughter DM, McDonough B, Wakimoto H, Gorham JM, Samari S, Mahbubani KT, Saeb-Parsy K, Patone G, Boyle JJ, Zhang H, Zhang H, Viveiros A, Oudit GY, Bayraktar OA, Seidman JG, Seidman CE, Noseda M, Hubner N, Teichmann SA. (2020) Cells of the adult human heart. Nature, 588(7838): 466-472.

30.   Brade T, Pane LS, Moretti A, Chien KR, Laugwitz KL. (2013) Embryonic heart progenitors and cardiogenesis. Cold Spring Harb Perspect Med, 3(10): a013847.

31.   Kehat I, Kenyagin-Karsenti D, Snir M, Segev H, Amit M, Gepstein A, Livne E, Binah O, Itskovitz-Eldor J, Gepstein L. (2001) Human embryonic stem cells can differentiate into myocytes with structural and functional properties of cardiomyocytes. J Clin Invest, 108(3): 407-414.

32.   Parikh A, Wu J, Blanton RM, Tzanakakis ES. (2015) Signaling Pathways and Gene Regulatory Networks in Cardiomyocyte Differentiation. Tissue Eng Part B Rev, 21(4): 377-392.

33.　Leitolis A, Robert AW, Pereira IT, Correa A, Stimamiglio MA. (2019) Cardiomyogenesis Modeling Using Pluripotent Stem Cells: The Role of Microenvironmental Signaling. Front Cell Dev Biol, 7: 164.

34.　Jha R, Xu RH, Xu C. (2015) Efficient differentiation of cardiomyocytes from human pluripotent stem cells with growth factors. Methods Mol Biol, 1299: 115-131.

35.　Lian X, Zhang J, Zhu K, Kamp TJ, Palecek SP. (2013) Insulin inhibits cardiac mesoderm, not mesendoderm, formation during cardiac differentiation of human pluripotent stem cells and modulation of canonical Wnt signaling can rescue this inhibition. Stem Cells, 31(3): 447-457.

36.　Zhao M, Tang Y, Zhou Y, Zhang J. (2019) Deciphering Role of Wnt Signalling in Cardiac Mesoderm and Cardiomyocyte Differentiation from Human iPSCs: Four-dimensional control of Wnt pathway for hiPSC-CMs differentiation. Sci Rep, 9(1): 19389.

37.　Minami I, Yamada K, Otsuji TG, Yamamoto T, Shen Y, Otsuka S, Kadota S, Morone N, Barve M, Asai Y, Tenkova-Heuser T, Heuser JE, Uesugi M, Aiba K, Nakatsuji N. (2012) A small molecule that promotes cardiac differentiation of human pluripotent stem cells under defined, cytokine- and xeno-free conditions. Cell Rep, 2(5): 1448-1460.

38.　Ban K, Bae S, Yoon YS. (2017) Current Strategies and Challenges for Purification of Cardiomyocytes Derived from Human Pluripotent Stem Cells. Theranostics, 7(7): 2067-2077.

39.　Zhao MT, Shao NY, Garg V. (2020) Subtype-specific cardiomyocytes for precision medicine: Where are we now? Stem Cells, 38(7): 822-833.

40.　Ahmed RE, Anzai T, Chanthra N, Uosaki H. (2020) A Brief Review of Current Maturation Methods for Human Induced Pluripotent Stem Cells-Derived Cardiomyocytes. Front Cell Dev Biol, 8: 178.

41.　Lopaschuk GD, Jaswal JS. (2010) Energy metabolic phenotype of the cardiomyocyte during development, differentiation, and postnatal maturation. J Cardiovasc Pharmacol, 56(2): 130-140.

42.　Morita Y, Tohyama S. (2020) Metabolic Regulation of Cardiac Differentiation and Maturation in Pluripotent Stem Cells: A Lesson from Heart Development. JMA J, 3(3): 193-200.

43.   Carlos-Oliveira M, Lozano-Juan F, Occhetta P, Visone R, Rasponi M. (2021) Current strategies of mechanical stimulation for maturation of cardiac microtissues. Biophys Rev, 13(5): 717-727.

44.   LaBarge W, Mattappally S, Kannappan R, Fast VG, Pretorius D, Berry JL, Zhang J. (2019) Maturation of three-dimensional, hiPSC-derived cardiomyocyte spheroids utilizing cyclic, uniaxial stretch and electrical stimulation. PLoS One, 14(7): e0219442.

45.   Shen N, Knopf A, Westendorf C, Kraushaar U, Riedl J, Bauer H, Poschel S, Layland SL, Holeiter M, Knolle S, Brauchle E, Nsair A, Hinderer S, Schenke-Layland K. (2017) Steps toward Maturation of Embryonic Stem Cell-Derived Cardiomyocytes by Defined Physical Signals. Stem Cell Reports, 9(1): 122-135.

46.   Parrotta EI, Lucchino V, Scaramuzzino L, Scalise S, Cuda G. (2020) Modeling Cardiac Disease Mechanisms Using Induced Pluripotent Stem Cell-Derived Cardiomyocytes: Progress, Promises and Challenges. Int J Mol Sci, 21(12).

47.   Hashimoto H, Olson EN, Bassel-Duby R. (2018) Therapeutic approaches for cardiac regeneration and repair. Nat Rev Cardiol, 15(10): 585-600.

48.   George RM, Maldonado-Velez G, Firulli AB. (2020) The heart of the neural crest: cardiac neural crest cells in development and regeneration. Development, 147(20).

49.   Srinivasan A, Toh YC. (2019) Human Pluripotent Stem Cell-Derived Neural Crest Cells for Tissue Regeneration and Disease Modeling. Front Mol Neurosci, 12: 39.

50.   Keyte A, Hutson MR. (2012) The neural crest in cardiac congenital anomalies. Differentiation, 84(1): 25-40.

51.   Erhardt S, Zheng M, Zhao X, Le TP, Findley TO, Wang J. (2021) The Cardiac Neural Crest Cells in Heart Development and Congenital Heart Defects. J Cardiovasc Dev Dis, 8(8).

52.   Chen W, Liu X, Li W, Shen H, Zeng Z, Yin K, Priest JR, Zhou Z. (2021) Single-cell transcriptomic landscape of cardiac neural crest cell derivatives during development. EMBO Rep, 22(11): e52389.

53.   Snarr BS, Kern CB, Wessels A. (2008) Origin and fate of cardiac mesenchyme. Dev Dyn, 237(10): 2804-2819.

54.   Brown CB, Baldwin HS. (2006) Neural crest contribution to the cardiovascular system. Adv Exp Med Biol, 589: 134-154.

55.   Arima Y, Miyagawa-Tomita S, Maeda K, Asai R, Seya D, Minoux M, Rijli FM, Nishiyama K, Kim KS, Uchijima Y, Ogawa H, Kurihara Y, Kurihara H. (2012) Preotic neural crest cells contribute to coronary artery smooth muscle involving endothelin signalling. Nat Commun, 3: 1267.

56.   Schleich JM, Abdulla T, Summers R, Houyel L. (2013) An overview of cardiac morphogenesis. Arch Cardiovasc Dis, 106(11): 612-623.

57.   Vega-Lopez GA, Cerrizuela S, Tribulo C, Aybar MJ. (2018) Neurocristopathies: New insights 150 years after the neural crest discovery. Dev Biol, 444 Suppl 1: S110-S143.

58.   Sato TS, Handa A, Priya S, Watal P, Becker RM, Sato Y. (2019) Neurocristopathies: Enigmatic Appearances of Neural Crest Cell-derived Abnormalities. Radiographics, 39(7): 2085-2102.

59.   Aljerian A, Gilardino MS. (2019) Treacher Collins Syndrome. Clin Plast Surg, 46(2): 197-205.

60.   Ma P, Gu S, Karunamuni GH, Jenkins MW, Watanabe M, Rollins AM. (2016) Cardiac neural crest ablation results in early endocardial cushion and hemodynamic flow abnormalities. Am J Physiol Heart Circ Physiol, 311(5): H1150-H1159.

61.   Waldo K, Zdanowicz M, Burch J, Kumiski DH, Stadt HA, Godt RE, Creazzo TL, Kirby ML. (1999) A novel role for cardiac neural crest in heart development. J Clin Invest, 103(11): 1499-1507.

62.   van den Hoff MJ, Moorman AF. (2000) Cardiac neural crest: the holy grail of cardiac abnormalities? Cardiovasc Res, 47(2): 212-216.

63.   Pomp O, Brokhman I, Ben-Dor I, Reubinoff B, Goldstein RS. (2005) Generation of peripheral sensory and sympathetic neurons and neural crest cells from human embryonic stem cells. Stem Cells, 23(7): 923-930.

64.   Lee G, Kim H, Elkabetz Y, Al Shamy G, Panagiotakos G, Barberi T, Tabar V, Studer L. (2007) Isolation and directed differentiation of neural crest stem cells derived from human embryonic stem cells. Nat Biotechnol, 25(12): 1468-1475.

65.   Kim YJ, Lim H, Li Z, Oh Y, Kovlyagina I, Choi IY, Dong X, Lee G. (2014) Generation of multipotent induced neural crest by direct reprogramming of human postnatal fibroblasts with a single transcription factor. Cell Stem Cell, 15(4): 497-506.

66.   Hackland JOS, Frith TJR, Thompson O, Marin Navarro A, Garcia-Castro MI, Unger C, Andrews PW. (2017) Top-Down Inhibition of BMP Signaling Enables Robust Induction of hPSCs Into Neural Crest in Fully Defined, Xeno-free Conditions. Stem Cell Reports, 9(4): 1043-1052.

67.   Pla P, Monsoro-Burq AH. (2018) The neural border: Induction, specification and maturation of the territory that generates neural crest cells. Dev Biol, 444 Suppl 1: S36-S46.

68.   Bajpai R, Chen DA, Rada-Iglesias A, Zhang J, Xiong Y, Helms J, Chang CP, Zhao Y, Swigut T, Wysocka J. (2010) CHD7 cooperates with PBAF to control multipotent neural crest formation. Nature, 463(7283): 958-962.

69.   Serrano F, Bernard WG, Granata A, Iyer D, Steventon B, Kim M, Vallier L, Gambardella L, Sinha S. (2019) A Novel Human Pluripotent Stem Cell-Derived Neural Crest Model of Treacher Collins Syndrome Shows Defects in Cell Death and Migration. Stem Cells Dev, 28(2): 81-100.

70.   Mica Y, Lee G, Chambers SM, Tomishima MJ, Studer L. (2013) Modeling neural crest induction, melanocyte specification, and disease-related pigmentation defects in hESCs and patient-specific iPSCs. Cell Rep, 3(4): 1140-1152.

71.   Huang M, Miller ML, McHenry LK, Zheng T, Zhen Q, Ilkhanizadeh S, Conklin BR, Bronner ME, Weiss WA. (2016) Generating trunk neural crest from human pluripotent stem cells. Sci Rep, 6: 19727.

72.   Shah AN, Gradishar WJ. (2018) Adjuvant Anthracyclines in Breast Cancer: What Is Their Role? The oncologist, 23(10): 1153-1161.

73.   Ghigo A, Li M, Hirsch E. (2016) New signal transduction paradigms in anthracycline-induced cardiotoxicity. Biochimica et biophysica acta, 1863(7 Pt B): 1916-1925.

74.   McGowan JV, Chung R, Maulik A, Piotrowska I, Walker JM, Yellon DM. (2017) Anthracycline Chemotherapy and Cardiotoxicity. Cardiovascular drugs and therapy, 31(1): 63-75.

75.   Burridge PW, Li YF, Matsa E, Wu H, Ong SG, Sharma A, Holmstrom A, Chang AC, Coronado MJ, Ebert AD, Knowles JW, Telli ML, Witteles RM, Blau HM, Bernstein D, Altman RB, Wu JC. (2016) Human induced pluripotent stem cell-derived cardiomyocytes

recapitulate the predilection of breast cancer patients to doxorubicin-induced cardiotoxicity. Nat Med, 22(5): 547-556.

76.   Kikuchi K, Poss KD. (2012) Cardiac regenerative capacity and mechanisms. Annual review of cell and developmental biology, 28: 719-741.

77.   Piccolo S, Dupont S, Cordenonsi M. (2014) The biology of YAP/TAZ: hippo signaling and beyond. Physiol Rev, 94(4): 1287-1312.

78.   Low BC, Pan CQ, Shivashankar GV, Bershadsky A, Sudol M, Sheetz M. (2014) YAP/TAZ as mechanosensors and mechanotransducers in regulating organ size and tumor growth. FEBS Lett, 588(16): 2663-2670.

79.   Cordenonsi M, Zanconato F, Azzolin L, Forcato M, Rosato A, Frasson C, Inui M, Montagner M, Parenti AR, Poletti A, Daidone MG, Dupont S, Basso G, Bicciato S, Piccolo S. (2011) The Hippo transducer TAZ confers cancer stem cell-related traits on breast cancer cells. Cell, 147(4): 759-772.

80.   Stanger BZ. (2012) Quit your YAPing: a new target for cancer therapy. Genes & development, 26(12): 1263-1267.

81.   Xu MZ, Yao TJ, Lee NP, Ng IO, Chan YT, Zender L, Lowe SW, Poon RT, Luk JM. (2009) Yes-associated protein is an independent prognostic marker in hepatocellular carcinoma. Cancer, 115(19): 4576-4585.

82.   Zhou Q, Li L, Zhao B, Guan KL. (2015) The hippo pathway in heart development, regeneration, and diseases. Circ Res, 116(8): 1431-1447.

83.   Windmueller R, Morrisey EE. (2015) Hippo and Cardiac Hypertrophy: A Complex Interaction. Circ Res, 117(10): 832-834.

84.   Mia MM, Singh MK. (2019) The Hippo Signaling Pathway in Cardiac Development and Diseases. Front Cell Dev Biol, 7: 211.

85.   Takaguri A, Akihiro O, Sasano J, Satoh K. (2020) Involvement of Yes-associated protein 1 (YAP1) in doxorubicin-induced cytotoxicity in H9c2 cardiac cells. Cell biology international, 44(3): 873-881.

86.   Li HR, Wang C, Sun P, Liu DD, Du GQ, Tian JW. (2020) Melatonin attenuates doxorubicin-induced cardiotoxicity through preservation of YAP expression. Journal of cellular and molecular medicine, 24(6): 3634-3646.

87.   Wang P, Wang M, Hu Y, Chen J, Cao Y, Liu C, Wu Z, Shen J, Lu J, Liu P. (2021) Isorhapontigenin protects against doxorubicin-induced cardiotoxicity via increasing YAP1 expression. Acta pharmaceutica Sinica B, 11(3): 680-693.

88.   Chen X, Li Y, Luo J, Hou N. (2020) Molecular Mechanism of Hippo-YAP1/TAZ Pathway in Heart Development, Disease, and Regeneration. Frontiers in physiology, 11: 389.

89.   Xiao D, Chang W, Ding W, Wang Y, Fa H, Wang J. (2020) Enhanced mitophagy mediated by the YAP/Parkin pathway protects against DOX-induced cardiotoxicity. Toxicology letters, 330: 96-107.

90.   Berecz T, Yiu A, Vittay O, Orsolits B, Mioulane M, Dos Remedios CG, Ketteler R, Merkely B, Apati A, Harding SE, Hellen N, Foldes G. (2021) Transcriptional co-activators YAP1-TAZ of Hippo signalling in doxorubicin-induced cardiomyopathy. ESC Heart Fail.

91.   Matsa E, Burridge PW, Yu KH, Ahrens JH, Termglinchan V, Wu H, Liu C, Shukla P, Sayed N, Churko JM, Shao N, Woo NA, Chao AS, Gold JD, Karakikes I, Snyder MP, Wu JC. (2016) Transcriptome Profiling of Patient-Specific Human iPSC-Cardiomyocytes Predicts Individual Drug Safety and Efficacy Responses In Vitro. Cell Stem Cell, 19(3): 311-325.

92.   McDonald-McGinn DM, Sullivan KE, Marino B, Philip N, Swillen A, Vorstman JA, Zackai EH, Emanuel BS, Vermeesch JR, Morrow BE, Scambler PJ, Bassett AS. (2015) 22q11.2 deletion syndrome. Nat Rev Dis Primers, 1: 15071.

93.   Du Q, de la Morena MT, van Oers NSC. (2019) The Genetics and Epigenetics of 22q11.2 Deletion Syndrome. Front Genet, 10: 1365.

94.   Kaushal D, Kalra N, Tyagi R, Khatri A, Biswas K. (2020) Pentalogy of Fallot: A case report and overview dental implications. Spec Care Dentist, 40(1): 121-126.

95.   Qin X, Chen J, Zhou T. (2020) 22q11.2 deletion syndrome and schizophrenia. Acta Biochim Biophys Sin (Shanghai), 52(11): 1181-1190.

96.   Khan TA, Revah O, Gordon A, Yoon SJ, Krawisz AK, Goold C, Sun Y, Kim CH, Tian Y, Li MY, Schaepe JM, Ikeda K, Amin ND, Sakai N, Yazawa M, Kushan L, Nishino S, Porteus MH, Rapoport JL, Bernstein JA, O'Hara R, Bearden CE, Hallmayer JF, Huguenard JR, Geschwind DH, Dolmetsch RE, Pasca SP. (2020) Neuronal defects in a human cellular model of 22q11.2 deletion syndrome. Nat Med, 26(12): 1888-1898.

97. Cirillo E, Giardino G, Gallo V, Puliafito P, Azzari C, Bacchetta R, Cardinale F, Cicalese MP, Consolini R, Martino S, Martire B, Molinatto C, Plebani A, Scarano G, Soresina A, Cancrini C, Rossi P, Digilio MC, Pignata C. (2014) Intergenerational and intrafamilial phenotypic variability in 22q11.2 deletion syndrome subjects. BMC Med Genet, 15: 1.

98. McDonald-McGinn DM. (2020) 22q11.2 deletion - a tiny piece leading to a big picture. Nat Rev Dis Primers, 6(1): 33.

99. Lindsay EA, Botta A, Jurecic V, Carattini-Rivera S, Cheah YC, Rosenblatt HM, Bradley A, Baldini A. (1999) Congenital heart disease in mice deficient for the DiGeorge syndrome region. Nature, 401(6751): 379-383.

100. Merscher S, Funke B, Epstein JA, Heyer J, Puech A, Lu MM, Xavier RJ, Demay MB, Russell RG, Factor S, Tokooya K, Jore BS, Lopez M, Pandita RK, Lia M, Carrion D, Xu H, Schorle H, Kobler JB, Scambler P, Wynshaw-Boris A, Skoultchi AI, Morrow BE, Kucherlapati R. (2001) TBX1 is responsible for cardiovascular defects in velo-cardio-facial/DiGeorge syndrome. Cell, 104(4): 619-629.

101. Stark KL, Xu B, Bagchi A, Lai WS, Liu H, Hsu R, Wan X, Pavlidis P, Mills AA, Karayiorgou M, Gogos JA. (2008) Altered brain microRNA biogenesis contributes to phenotypic deficits in a 22q11-deletion mouse model. Nat Genet, 40(6): 751-760.

102. Saito R, Koebis M, Nagai T, Shimizu K, Liao J, Wulaer B, Sugaya Y, Nagahama K, Uesaka N, Kushima I, Mori D, Maruyama K, Nakao K, Kurihara H, Yamada K, Kano M, Fukada Y, Ozaki N, Aiba A. (2020) Comprehensive analysis of a novel mouse model of the 22q11.2 deletion syndrome: a model with the most common 3.0-Mb deletion at the human 22q11.2 locus. Transl Psychiatry, 10(1): 35.

103. Pane LS, Fulcoli FG, Cirino A, Altomonte A, Ferrentino R, Bilio M, Baldini A. (2018) Tbx1 represses Mef2c gene expression and is correlated with histone 3 deacetylation of the anterior heart field enhancer. Dis Model Mech, 11(9).

104. Drew LJ, Crabtree GW, Markx S, Stark KL, Chaverneff F, Xu B, Mukai J, Fenelon K, Hsu PK, Gogos JA, Karayiorgou M. (2011) The 22q11.2 microdeletion: fifteen years of insights into the genetic and neural complexity of psychiatric disorders. Int J Dev Neurosci, 29(3): 259-281.

105.   Zhao D, Lin M, Chen J, Pedrosa E, Hrabovsky A, Fourcade HM, Zheng D, Lachman HM. (2015) MicroRNA Profiling of Neurons Generated Using Induced Pluripotent Stem Cells Derived from Patients with Schizophrenia and Schizoaffective Disorder, and 22q11.2 Del. PLoS One, 10(7): e0132387.

106.   Toyoshima M, Akamatsu W, Okada Y, Ohnishi T, Balan S, Hisano Y, Iwayama Y, Toyota T, Matsumoto T, Itasaka N, Sugiyama S, Tanaka M, Yano M, Dean B, Okano H, Yoshikawa T. (2016) Analysis of induced pluripotent stem cells carrying 22q11.2 deletion. Transl Psychiatry, 6(11): e934.

107.   Lin M, Pedrosa E, Hrabovsky A, Chen J, Puliafito BR, Gilbert SR, Zheng D, Lachman HM. (2016) Integrative transcriptome network analysis of iPSC-derived neurons from schizophrenia and schizoaffective disorder patients with 22q11.2 deletion. BMC Syst Biol, 10(1): 105.

108.   Motahari Z, Moody SA, Maynard TM, LaMantia AS. (2019) In the line-up: deleted genes associated with DiGeorge/22q11.2 deletion syndrome: are they all suspects? J Neurodev Disord, 11(1): 7.

109.   Li J, Ryan SK, Deboer E, Cook K, Fitzgerald S, Lachman HM, Wallace DC, Goldberg EM, Anderson SA. (2019) Mitochondrial deficits in human iPSC-derived neurons from patients with 22q11.2 deletion syndrome and schizophrenia. Transl Psychiatry, 9(1): 302.

110.   Jurata LW, Gallagher P, Lemire AL, Charles V, Brockman JA, Illingworth EL, Altar CA. (2006) Altered expression of hippocampal dentate granule neuron genes in a mouse model of human 22q11 deletion syndrome. Schizophr Res, 88(1-3): 251-259.

111.   Drew LJ, Stark KL, Fenelon K, Karayiorgou M, Macdermott AB, Gogos JA. (2011) Evidence for altered hippocampal function in a mouse model of the human 22q11.2 microdeletion. Mol Cell Neurosci, 47(4): 293-305.

112.   Eriksson PS, Perfilieva E, Bjork-Eriksson T, Alborn AM, Nordborg C, Peterson DA, Gage FH. (1998) Neurogenesis in the adult human hippocampus. Nat Med, 4(11): 1313-1317.

113.   Boldrini M, Fulmore CA, Tartt AN, Simeon LR, Pavlova I, Poposka V, Rosoklija GB, Stankov A, Arango V, Dwork AJ, Hen R, Mann JJ. (2018) Human Hippocampal Neurogenesis Persists throughout Aging. Cell Stem Cell, 22(4): 589-599 e585.

114.   Zhao C, Deng W, Gage FH. (2008) Mechanisms and functional implications of adult neurogenesis. Cell, 132(4): 645-660.

115.   Reif A, Fritzen S, Finger M, Strobel A, Lauer M, Schmitt A, Lesch KP. (2006) Neural stem cell proliferation is decreased in schizophrenia, but not in depression. Mol Psychiatry, 11(5): 514-522.

116.   Tamminga CA, Stan AD, Wagner AD. (2010) The hippocampal formation in schizophrenia. Am J Psychiatry, 167(10): 1178-1193.

117.   Walton NM, Zhou Y, Kogan JH, Shin R, Webster M, Gross AK, Heusner CL, Chen Q, Miyake S, Tajinda K, Tamura K, Miyakawa T, Matsumoto M. (2012) Detection of an immature dentate gyrus feature in human schizophrenia/bipolar patients. Transl Psychiatry, 2: e135.

118.   Hagihara H, Takao K, Walton NM, Matsumoto M, Miyakawa T. (2013) Immature dentate gyrus: an endophenotype of neuropsychiatric disorders. Neural Plast, 2013: 318596.

119.   Shin R, Kobayashi K, Hagihara H, Kogan JH, Miyake S, Tajinda K, Walton NM, Gross AK, Heusner CL, Chen Q, Tamura K, Miyakawa T, Matsumoto M. (2013) The immature dentate gyrus represents a shared phenotype of mouse models of epilepsy and psychiatric disease. Bipolar Disord, 15(4): 405-421.

120.   Jessberger S, Zhao C, Toni N, Clemenson GD, Jr., Li Y, Gage FH. (2007) Seizure-associated, aberrant neurogenesis in adult rats characterized with retrovirus-mediated cell labeling. J Neurosci, 27(35): 9400-9407.

121.   Tatebayashi Y, Lee MH, Li L, Iqbal K, Grundke-Iqbal I. (2003) The dentate gyrus neurogenesis: a therapeutic target for Alzheimer's disease. Acta Neuropathol, 105(3): 225-232.

122.   Sahay A, Hen R. (2008) Hippocampal neurogenesis and depression. Novartis Found Symp, 289: 152-160; discussion 160-154, 193-155.

123.   Mateus-Pinheiro A, Pinto L, Bessa JM, Morais M, Alves ND, Monteiro S, Patricio P, Almeida OF, Sousa N. (2013) Sustained remission from depressive-like behavior depends on hippocampal neurogenesis. Transl Psychiatry, 3: e210.

124.   Kozubenko N, Turnovcova K, Kapcalova M, Butenko O, Anderova M, Rusnakova V, Kubista M, Hampl A, Jendelova P, Sykova E. (2010) Analysis of in vitro and in vivo

characteristics of human embryonic stem cell-derived neural precursors. Cell Transplant, 19(4): 471-486.

125.   Kim YS, Park CH. (2011) Dopamine neuron generation from human embryonic stem cells. Int J Stem Cells, 4(2): 85-87.

126.   Li W, Sun W, Zhang Y, Wei W, Ambasudhan R, Xia P, Talantova M, Lin T, Kim J, Wang X, Kim WR, Lipton SA, Zhang K, Ding S. (2011) Rapid induction and long-term self-renewal of primitive neural precursors from human embryonic stem cells by small molecule inhibitors. Proc Natl Acad Sci U S A, 108(20): 8299-8304.

127.   Forostyak O, Romanyuk N, Verkhratsky A, Sykova E, Dayanithi G. (2013) Plasticity of calcium signaling cascades in human embryonic stem cell-derived neural precursors. Stem Cells Dev, 22(10): 1506-1521.

128.   Viero C, Forostyak O, Sykova E, Dayanithi G. (2014) Getting it right before transplantation: example of a stem cell model with regenerative potential for the CNS. Front Cell Dev Biol, 2: 36.

129.   Yu DX, Di Giorgio FP, Yao J, Marchetto MC, Brennand K, Wright R, Mei A, McHenry L, Lisuk D, Grasmick JM, Silberman P, Silberman G, Jappelli R, Gage FH. (2014) Modeling hippocampal neurogenesis using human pluripotent stem cells. Stem Cell Reports, 2(3): 295-310.

130.   Stergiopoulos A, Elkouris M, Politis PK. (2014) Prospero-related homeobox 1 (Prox1) at the crossroads of diverse pathways during adult neural fate specification. Front Cell Neurosci, 8: 454.

131.   Iwano T, Masuda A, Kiyonari H, Enomoto H, Matsuzaki F. (2012) Prox1 postmitotically defines dentate gyrus cells by specifying granule cell identity over CA3 pyramidal cell fate in the hippocampus. Development, 139(16): 3051-3062.

132.   Mertens J, Wang QW, Kim Y, Yu DX, Pham S, Yang B, Zheng Y, Diffenderfer KE, Zhang J, Soltani S, Eames T, Schafer ST, Boyer L, Marchetto MC, Nurnberger JI, Calabrese JR, Odegaard KJ, McCarthy MJ, Zandi PP, Alda M, Nievergelt CM, Pharmacogenomics of Bipolar Disorder S, Mi S, Brennand KJ, Kelsoe JR, Gage FH, Yao J. (2015) Differential responses to lithium in hyperexcitable neurons from patients with bipolar disorder. Nature, 527(7576): 95-99.

133.   Malmersjo S, Liste I, Dyachok O, Tengholm A, Arenas E, Uhlen P. (2010) Ca2+ and cAMP signaling in human embryonic stem cell-derived dopamine neurons. Stem Cells Dev, 19(9): 1355-1364.

134.   Chen TW, Wardill TJ, Sun Y, Pulver SR, Renninger SL, Baohan A, Schreiter ER, Kerr RA, Orger MB, Jayaraman V, Looger LL, Svoboda K, Kim DS. (2013) Ultrasensitive fluorescent proteins for imaging neuronal activity. Nature, 499(7458): 295-300.

135.   Malmersjo S, Rebellato P, Smedler E, Planert H, Kanatani S, Liste I, Nanou E, Sunner H, Abdelhady S, Zhang S, Andang M, El Manira A, Silberberg G, Arenas E, Uhlen P. (2013) Neural progenitors organize in small-world networks to promote cell proliferation. Proc Natl Acad Sci U S A, 110(16): E1524-1532.

136.   Smedler E, Malmersjo S, Uhlen P. (2014) Network analysis of time-lapse microscopy recordings. Front Neural Circuits, 8: 111.

137.   North RA. (2002) Molecular physiology of P2X receptors. Physiol Rev, 82(4): 1013-1067.

138.   von Kugelgen I, Harden TK. (2011) Molecular pharmacology, physiology, and structure of the P2Y receptors. Adv Pharmacol, 61: 373-415.

139.   Contos JJ, Ishii I, Chun J. (2000) Lysophosphatidic acid receptors. Mol Pharmacol, 58(6): 1188-1196.

140.   O'Brien PJ, Molino M, Kahn M, Brass LF. (2001) Protease activated receptors: theme and variations. Oncogene, 20(13): 1570-1581.

141.   Radeff-Huang J, Seasholtz TM, Matteo RG, Brown JH. (2004) G protein mediated signaling pathways in lysophospholipid induced cell proliferation and survival. J Cell Biochem, 92(5): 949-966.

142.   Mikoshiba K. (2015) Role of IP3 receptor signaling in cell functions and diseases. Adv Biol Regul, 57: 217-227.

143.   Philippe R, Antigny F, Buscaglia P, Norez C, Becq F, Frieden M, Mignen O. (2015) SERCA and PMCA pumps contribute to the deregulation of Ca2+ homeostasis in human CF epithelial cells. Biochimica et biophysica acta, 1853(5): 892-903.

144.   Kawano S, Shoji S, Ichinose S, Yamagata K, Tagami M, Hiraoka M. (2002) Characterization of Ca(2+) signaling pathways in human mesenchymal stem cells. Cell Calcium, 32(4): 165-174.

145. Giladi M, Tal I, Khananshvili D. (2016) Structural Features of Ion Transport and Allosteric Regulation in Sodium-Calcium Exchanger (NCX) Proteins. Frontiers in physiology, 7: 30.

146. Raingo J, Rebolledo A, Iveli F, Grassi de Gende AO, Milesi V. (2004) Non-selective cationic channels (NSCC) in smooth muscle cells from human umbilical arteries. Placenta, 25(8-9): 723-729.

147. Dolphin AC. (2006) A short history of voltage-gated calcium channels. Br J Pharmacol, 147 Suppl 1: S56-62.

148. Kirichok Y, Krapivinsky G, Clapham DE. (2004) The mitochondrial calcium uniporter is a highly selective ion channel. Nature, 427(6972): 360-364.

149. Nicolau SM, Egea J, Lopez MG, Garcia AG. (2010) Mitochondrial Na+/Ca2+ exchanger, a new target for neuroprotection in rat hippocampal slices. Biochem Biophys Res Commun, 400(1): 140-144.

150. Mauger JP. (2012) Role of the nuclear envelope in calcium signalling. Biol Cell, 104(2): 70-83.

151. Hertle DN, Yeckel MF. (2007) Distribution of inositol-1,4,5-trisphosphate receptor isotypes and ryanodine receptor isotypes during maturation of the rat hippocampus. Neuroscience, 150(3): 625-638.

152. Hu H, Wang Z, Wei R, Fan G, Wang Q, Zhang K, Yin CC. (2015) The molecular architecture of dihydropyrindine receptor/L-type Ca2+ channel complex. Sci Rep, 5: 8370.

153. Adasme T, Paula-Lima A, Hidalgo C. (2015) Inhibitory ryanodine prevents ryanodine receptor-mediated Ca(2)(+) release without affecting endoplasmic reticulum Ca(2)(+) content in primary hippocampal neurons. Biochem Biophys Res Commun, 458(1): 57-62.

154. Futagi D, Kitano K. (2015) Ryanodine-receptor-driven intracellular calcium dynamics underlying spatial association of synaptic plasticity. J Comput Neurosci, 39(3): 329-347.

155. Amaral DG, Scharfman HE, Lavenex P. (2007) The dentate gyrus: fundamental neuroanatomical organization (dentate gyrus for dummies). Prog Brain Res, 163: 3-22.

156. Yu DX, Marchetto MC, Gage FH. (2014) How to make a hippocampal dentate gyrus granule neuron. Development, 141(12): 2366-2375.

157.   Fukushima K, Tabata Y, Imaizumi Y, Kohmura N, Sugawara M, Sawada K, Yamazaki K, Ito M. (2014) Characterization of Human Hippocampal Neural Stem/Progenitor Cells and Their Application to Physiologically Relevant Assays for Multiple Ionotropic Glutamate Receptors. J Biomol Screen, 19(8): 1174-1184.

158.   Bernabeu R, Sharp FR. (2000) NMDA and AMPA/kainate glutamate receptors modulate dentate neurogenesis and CA3 synapsin-I in normal and ischemic hippocampus. J Cereb Blood Flow Metab, 20(12): 1669-1680.

159.   Antal M, Fukazawa Y, Eordogh M, Muszil D, Molnar E, Itakura M, Takahashi M, Shigemoto R. (2008) Numbers, densities, and colocalization of AMPA- and NMDA-type glutamate receptors at individual synapses in the superficial spinal dorsal horn of rats. J Neurosci, 28(39): 9692-9701.

160.   Karhu ST, Kinnunen SM, Tolli M, Valimaki MJ, Szabo Z, Talman V, Ruskoaho H. (2020) GATA4-targeted compound exhibits cardioprotective actions against doxorubicin-induced toxicity in vitro and in vivo: establishment of a chronic cardiotoxicity model using human iPSC-derived cardiomyocytes. Arch Toxicol, 94(6): 2113-2130.

161.   Berecz T, Husveth-Toth M, Mioulane M, Merkely B, Apati A, Foldes G. (2020) Generation and Analysis of Pluripotent Stem Cell-Derived Cardiomyocytes and Endothelial Cells for High Content Screening Purposes. Methods Mol Biol, 2150: 57-77.

162.   Vofely G, Berecz T, Szabo E, Szebenyi K, Hathy E, Orban TI, Sarkadi B, Homolya L, Marchetto MC, Rethelyi JM, Apati A. (2018) Characterization of calcium signals in human induced pluripotent stem cell-derived dentate gyrus neuronal progenitors and mature neurons, stably expressing an advanced calcium indicator protein. Mol Cell Neurosci, 88: 222-230.

163.   Lugli E, Troiano L, Ferraresi R, Roat E, Prada N, Nasi M, Pinti M, Cooper EL, Cossarizza A. (2005) Characterization of cells with different mitochondrial membrane potential during apoptosis. Cytometry A, 68(1): 28-35.

164.   Saraste A, Pulkki K. (2000) Morphologic and biochemical hallmarks of apoptosis. Cardiovasc Res, 45(3): 528-537.

165.   Rausch V, Hansen CG. (2020) The Hippo Pathway, YAP/TAZ, and the Plasma Membrane. Trends Cell Biol, 30(1): 32-48.

166. Aragona M, Panciera T, Manfrin A, Giulitti S, Michielin F, Elvassore N, Dupont S, Piccolo S. (2013) A mechanical checkpoint controls multicellular growth through YAP/TAZ regulation by actin-processing factors. Cell, 154(5): 1047-1059.

167. Pavel M, Renna M, Park SJ, Menzies FM, Ricketts T, Fullgrabe J, Ashkenazi A, Frake RA, Lombarte AC, Bento CF, Franze K, Rubinsztein DC. (2018) Contact inhibition controls cell survival and proliferation via YAP/TAZ-autophagy axis. Nat Commun, 9(1): 2961.

168. Karaman R, Halder G. (2018) Cell Junctions in Hippo Signaling. Cold Spring Harb Perspect Biol, 10(5).

169. Riveros Gilardi B, Munoz Lopez JI, Hernandez Villegas AC, Garay Mora JA, Rico Rodriguez OC, Chavez Appendini R, De la Mora Malvaez M, Higuera Calleja JA. (2019) Types of Cerebral Herniation and Their Imaging Features. Radiographics, 39(6): 1598-1610.

170. Wilch ES, Morton CC. (2018) Historical and Clinical Perspectives on Chromosomal Translocations. Adv Exp Med Biol, 1044: 1-14.

171. Burridge PW, Holmstrom A, Wu JC. (2015) Chemically Defined Culture and Cardiomyocyte Differentiation of Human Pluripotent Stem Cells. Curr Protoc Hum Genet, 87: 21 23 21-21 23 15.

172. Lee JH, Protze SI, Laksman Z, Backx PH, Keller GM. (2017) Human Pluripotent Stem Cell-Derived Atrial and Ventricular Cardiomyocytes Develop from Distinct Mesoderm Populations. Cell Stem Cell, 21(2): 179-194 e174.

173. Salameh A, Blanke K, Daehnert I. (2013) Role of connexins in human congenital heart disease: the chicken and egg problem. Front Pharmacol, 4: 70.

174. Smedler E, Uhlen P. (2014) Frequency decoding of calcium oscillations. Biochimica et biophysica acta, 1840(3): 964-969.

175. Ali F, Kwan AC. (2020) Interpreting in vivo calcium signals from neuronal cell bodies, axons, and dendrites: a review. Neurophotonics, 7(1): 011402.

176. Han Y. (2019) Analysis of the role of the Hippo pathway in cancer. J Transl Med, 17(1): 116.

177. Johnson R, Halder G. (2014) The two faces of Hippo: targeting the Hippo pathway for regenerative medicine and cancer treatment. Nat Rev Drug Discov, 13(1): 63-79.

178.   Zhang H, Yu QL, Meng L, Huang H, Liu H, Zhang N, Liu N, Yang J, Zhang YZ, Huang Q. (2020) TAZ-regulated expression of IL-8 is involved in chemoresistance of hepatocellular carcinoma cells. Arch Biochem Biophys, 693: 108571.

179.   Huo X, Zhang Q, Liu AM, Tang C, Gong Y, Bian J, Luk JM, Xu Z, Chen J. (2013) Overexpression of Yes-associated protein confers doxorubicin resistance in hepatocellullar carcinoma. Oncol Rep, 29(2): 840-846.

180.   Golforoush PA, Narasimhan P, Chaves-Guerrero PP, Lawrence E, Newton G, Yan R, Harding SE, Perrior T, Chapman KL, Schneider MD. (2020) Selective protection of human cardiomyocytes from anthracycline cardiotoxicity by small molecule inhibitors of MAP4K4. Sci Rep, 10(1): 12060.

181.   Lin Z, von Gise A, Zhou P, Gu F, Ma Q, Jiang J, Yau AL, Buck JN, Gouin KA, van Gorp PR, Zhou B, Chen J, Seidman JG, Wang DZ, Pu WT. (2014) Cardiac-specific YAP activation improves cardiac function and survival in an experimental murine MI model. Circ Res, 115(3): 354-363.

182.   ten Velde I, de Jonge B, Verheijck EE, van Kempen MJ, Analbers L, Gros D, Jongsma HJ. (1995) Spatial distribution of connexin43, the major cardiac gap junction protein, visualizes the cellular network for impulse propagation from sinoatrial node to atrium. Circ Res, 76(5): 802-811.

183.   Salameh A, Haunschild J, Brauchle P, Peim O, Seidel T, Reitmann M, Kostelka M, Bakhtiary F, Dhein S, Dahnert I. (2014) On the role of the gap junction protein Cx43 (GJA1) in human cardiac malformations with Fallot-pathology. a study on paediatric cardiac specimen. PLoS One, 9(4): e95344.

184.   Schock EN, LaBonne C. (2020) Sorting Sox: Diverse Roles for Sox Transcription Factors During Neural Crest and Craniofacial Development. Frontiers in physiology, 11: 606889.

185.   McKeown SJ, Lee VM, Bronner-Fraser M, Newgreen DF, Farlie PG. (2005) Sox10 overexpression induces neural crest-like cells from all dorsoventral levels of the neural tube but inhibits differentiation. Dev Dyn, 233(2): 430-444.

186.   Cheung M, Chaboissier MC, Mynett A, Hirst E, Schedl A, Briscoe J. (2005) The transcriptional control of trunk neural crest induction, survival, and delamination. Dev Cell, 8(2): 179-192.

187.   Liu JA, Wu MH, Yan CH, Chau BK, So H, Ng A, Chan A, Cheah KS, Briscoe J, Cheung M. (2013) Phosphorylation of Sox9 is required for neural crest delamination and is regulated downstream of BMP and canonical Wnt signaling. Proc Natl Acad Sci U S A, 110(8): 2882-2887.

188.   Wang WD, Melville DB, Montero-Balaguer M, Hatzopoulos AK, Knapik EW. (2011) Tfap2a and Foxd3 regulate early steps in the development of the neural crest progenitor population. Dev Biol, 360(1): 173-185.

189.   de Croze N, Maczkowiak F, Monsoro-Burq AH. (2011) Reiterative AP2a activity controls sequential steps in the neural crest gene regulatory network. Proc Natl Acad Sci U S A, 108(1): 155-160.

190.   Peyton L, Oliveros A, Choi DS, Jang MH. (2021) Hippocampal regenerative medicine: neurogenic implications for addiction and mental disorders. Exp Mol Med, 53(3): 358-368.

8. Bibliography of the candidate's publication

8.1. Publications related to the PhD thesis

1. **Berecz T**, Yiu A, Vittay O, Orsolits B, Mioulane M, Dos Remedios CG, Ketteler R, Merkely B, Apati A, Harding SE, Hellen N, Foldes G. (2021) Transcriptional co-activators YAP1-TAZ of Hippo signalling in doxorubicin-induced cardiomyopathy. ESC Heart Fail, 9(1): 224-235. **IF: 4.411**

2. **Berecz T**, Husveth-Toth M, Mioulane M, Merkely B, Apati A, Foldes G. (2020) Generation and Analysis of Pluripotent Stem Cell-Derived Cardiomyocytes and Endothelial Cells for High Content Screening Purposes. Methods Mol Biol, 2150: 57-77.

3. Vofely G, **Berecz T**, Szabo E, Szebenyi K, Hathy E, Orban TI, Sarkadi B, Homolya L, Marchetto MC, Rethelyi JM, Apati A. (2018) Characterization of calcium signals in human induced pluripotent stem cell-derived dentate gyrus neuronal progenitors and mature neurons, stably expressing an advanced calcium indicator protein. Mol Cell Neurosci. 88: 222-230. **IF: 2.855**

8.2. Other publications

1. Izadifar M, **Berecz T**, Apati A, Nagy A. (2021) An Optical-Flow-Based Method to Quantify Dynamic Behavior of Human Pluripotent Stem Cell-Derived Cardiomyocytes in Disease Modeling Platforms. Methods Mol Biol. (doi: 10.1007/7651_2021_382)

2. Apati A, Varga N, **Berecz T**, Erdei Z, Homolya L, Sarkadi B. (2019) Application of human pluripotent stem cells and pluripotent stem cell-derived cellular models for assessing drug toxicity. Expert Opin Drug Metab Toxicol, 15(1): 61-75. **IF: 3.47**

3. Blacker TS, **Berecz T**, Duchen MR, Szabadkai G. (2017) Assessment of Cellular Redox State Using NAD(P)H Fluorescence Intensity and Lifetime. Bio Protoc, 7(2): e2105.

4. Tosatto A, Sommaggio R, Kummerow C, Bentham RB, Blacker TS, **Berecz T**, Duchen MR, Rosato A, Bogeski I, Szabadkai G, Rizzuto R, Mammucari C. (2016) The mitochondrial calcium uniporter regulates breast cancer progression via HIF-1alpha. EMBO Mol Med, 8: 569-585. **IF: 9,249**

5. Apati A, **Berecz T**, Sarkadi B. (2016) Calcium signaling in human pluripotent stem cells. Cell Calcium, 59: 117-123. **IF: 3.707**

9. Acknowledgements

Supplementary material

Table of detailed clinical symptoms of the family members

	Child phenotype	Mother phenotype	Grandfather phenotype	Father phenotype	Grandmother phenotype
Cardiovascular system					
pulmonary atresia	+				
ventricular septal defect	+				
atrial septal defect type ii	+				
right aortic arch with aberrant left subclavian artery	+				
stenosis of aortopulmonary collateral arteries	+				
vascular ring		+			
MRI / CT / Echocardiography readouts					
third-degree atrioventricular block arrhythmia /conduction disorders	+				
Neuropsychological system					
Dysarthria	N/A		+		
learning disability	N/A				
language development delay	N/A				
Neurodevelopmental delay	N/A				
Hypernasal tone of voice					
ventricular asymmetry	+				
Thymus					
T-cell defficiency	+	+			
recurrent infections	+	+			
thymic alterations (hypoplasia/aplasia)?					
Immunodeficiency by laboratory analysis?					
Parathyroid gland					
hypocalcaemia to hypoparathyroidism		+			
Renal system					
pyelectasia l.d.	+				
medullary sponge kidney		+			
hypercalciuria		+			
Craniofacial-skeletal system					
facial anomaly	+	+	+		
micrognathia	+				
long face					
hooded eyelids					
tubular nose					
alar hypoplasia					
velopharyngeal insufficiency					
overt or submucous cleft palate			+		
cleft lip/palate					
Other					
anaemia	+	+			
hyperthyroidism			+		
Inguinal hernia			+		